IN VIVO RAT MODELS OF BRAIN β-AMYLOID PATHOLOGY

Department of Medical Chemistry

University of Szeged

PhD. Thesis

Eszter Sipos

Supervisors:
Zsuzsa Penke, Ph. D.
Professor Botond Penke, Ph. D.

Szeged
2009.

1 CONTENTS

2 LIST OF PUBLICATIONS

2.1 Full papers, directly related to the subject of the thesis

- **β-Amyloid pathology in the entorhinal cortex in rats contributes to the memory deficits associated with Alzheimer's disease**
  E. Sipos, A. Kurunczi, Á. Kasza, J. Horváth, K. Felszeghy, S. Laroche, J. Toldi, Á. Párducz, B. Penke, Zs. Penke. Neuroscience, (2007), 147(1): 28-36 (IF:3,35)

- **Intranasal Delivery of Human β-Amyloid Peptide in Rats: Effective brain targeting**
  E. Sipos, A. Kurunczi, A. Fehér, Z. Penke, L. Fülöp, Á. Kasza, J. Horvát, S. Horvat, Sz. Veszelka, G. Balogh, L. Kürti, I. Erős, P. Szabó-Révész, Á. Párducz, B. Penke, M. A. Deli Cell Mol Neurosci, (2009), in press (DOI: 10.1007/s10571-009-9463-6) (IF:2,55)

2.2 Lectures at congresses

- **Rodent models of Alzheimer disease, measuring behavioural changing and memory deficits.** X. Hungarian Alzheimer Congress; Szeged, Hungary Sept. 2006.

2.3 Posters

- **Histological changes in Entorhinal cortex induced by beta-amyloid in a rat model**
  J. Horváth, **E. Sipos**, A. Kurunczi, Zs. Penke, Á. Kasza, B. Penke. X. Hungarian Alzheimer Congress; Szeged, Hungary Sept. 2006.
- **Intranasal delivery of human beta-amyloid peptides in rats: towards a new model of Alzheimer's disease**
  A. Kurunczi , A. Fehér, **E. Sipos-Bodó**, Sz. Veszelka, P. Szabó-Révész, I. Erős, Á. Párducz, B. Penke, M. Deli. X. Hungarian Alzheimer Congress; Szeged, Hungary Sept. 2006.
- **Intranasal delivery of human beta-amyloid peptides in rats: towards a new model of Alzheimer's disease**
  A. Kurunczi , A. S. Fehér , **E. Sipos-Bodó**, Sz. Veszelka, S. H., P. Szabó-Révész, I. Erős, Á. Párducz, B. Penke, M. Deli. 5th FENS Wien, Austria Jul. 2006
- **A potential in vivo rat model of the Alzeimer's disease**
  E. Sipos-Bodó, Zs.Penke, A. Kurunczi, K. Felszeghy, B. Penke. 5th FENS Wien, Austria Jul. 2006
- **Evaluation of memory deficit induced by beta-amyloid in a rat model**
  E. Sipos-Bodó, A Kurunczi, Á. Kasza, J.Horváth, K. Felszeghy, Zs. Penke, Á. Párducz, J. Toldi, B. Penke. The 4th Kuopio Alzheimer Symposium, Kuopio, Finland Feb. 2006
- **Evaluation of memory deficit induced by beta-amyloid in a rat model**
  E. Sipos-Bodó, A Kurunczi, Á. Kasza, J.Horváth, K. Felszeghy, Zs. Penke, Á. Párducz, J. Toldi, B. Penke. IBRO Budapest, Hungary Jan. 2006
- **Evaluation of memory deficit induced by beta-amyloid in a rat model**
  E. Sipos, E. Borbély, Zs. Penke, A. Kurunczi, J. Toldi, B. Penke. IX. Hungarian Alzheimer Congress; Kecskemét, Hungary Sept. 2005

3 ABBREVIATIONS

AchE	acetylcholine esterase
AD	Alzheimer's disease
AMCA	7-amino-4-methyl-3-coumarinylacetic acid
ApoE	apolipoprotein-E
APP	amyloid precursor protein
Aβ	amyloid beta
BBB	blood-brain-barrier
CA	cornu Ammonis
ChAT	cholin acetyl transferase
CNS	central nervous system
CSF	cerebrospinal fluid
DG	gyrus dentatus
EC	entorhinal cortex
ELISA	enzyme-linked immunoabsorbent assay
GFAP	glial fibrillary acidic protein
HC	hippocampus
IR	immunoreactivity
MTL	medial temporal lobe
NFT	neurofibrillary tangles
NMDA	N-metil-D-aspartate
PBS	phosphate-buffered saline
PS1	presenilin1
PS2	presenilin2
SAMP8	senescence-accelerated mouse prone/8
TBS	tris-buffered salin

4 SUMMARY

Alzheimer's disease (AD) is the most common cause of dementia in humans. There is a widespread interest in the development of AD models, as a way to better understand and treat the disease. The main aim of this thesis was to develop simple, easy and cost-effective animal models of AD that could be suitable for drug testing purposes. One of the underlying pathological causes of AD is the accumulation of amyloid beta (Aβ), therefore we based our models on this molecule.

Our first model consisted of injecting Aβ into the entorhinal cortex (EC). EC was chosen as a target because it is one of the first brain regions where amyloid plaques appear in AD, however, the effects of Aβ injection into this area have not been studied. In the present study, the neurotoxic effects of Aβ injections were demonstrated with behavioral and histological methods. We concluded that entorhinal Aβ injection was a suitable model for several aspects of early AD.

In our second model, Aβ1-42 peptide was administered intranasally to rats. Our main aim was to develop a unique, non-invasive model allowing direct administration of Aβ into the brain. This nasal administration procedure of Aβ1-42 offers an alternative route to CNS circumventing blood-brain barrier in rats. A special nasal vehicle was used, which increases the brain transport of the test molecule. We showed that intranasal Aβ administration induces learning impairment and morphological alterations characteristic of AD, especially in the olfactory bulb and frontal cortex regions. In conclusion, nasal administration of Aβ could be a potential model of AD. Moreover, the nasal pathway has a potential for targeting therapeutical drugs for AD to the central nervous system.

5 INTRODUCTION

5.1 Alzheimer's disease

5.1.1 General description

Alzheimer's disease (AD) is the most common cause of dementia (defined as an impairment of memory and cognitive function) in humans, affecting mainly elderly people. It is a neurodegenerative disorder characterized by progressive cognitive deterioration (disorientation, confusion and problems with reasoning), behavioral disturbances (agitation, anxiety, delusions, depression and insomnia) and a devastating memory loss (Kar et al. 2004). Neuropathological stages of AD and related changes were first published by Braak and Braak (1991). Up to now, the problem of treating and curing of AD has not been solved, although several medication methods have been used (Andrade and Radhakrishnan 2009).

Alzheimer's disease pathology may be divided into three broad chapters. Positive lesions – lesions related to accumulation – are the main neuropathological hallmarks of AD, mainly constituted by the extracellular deposition of amyloid beta peptide and the intracellular aggregation of tau protein. Negative lesions – loss of neurons and synapses – are difficult to evaluate; they do not belong to the diagnostic criteria but could be the alterations that are more directly related to the cognitive deficit. The third type of lesions is due to reactive processes: inflammation and altered regenerative processes (Duyckaerts et al. 2009).

The pathology of AD and other tauopathies was discussed by Iqbal et al. (2005; 2009). A most recent publication of Mucke (2009) provides an excellent summary of our knowledge of AD.

5.1.2 Accumulation of the tau protein

Neurofibrillary tangles consist of paired helical fragments composed of the hyperphosphorylated form of microtubule-associated tau protein (Selkoe 2001; Dodart and May 2005). Ultrastructurally, these fibres consist of pairs of approximately 10 nm filaments wound into helices with a helical period of ~160 nm as revealed by electron microscopy. The normal function of the tau protein is microtubule binding and stabilizing. In AD, the

reversible enzymatically mediated dephosphorylation is impaired, and the resulting hyperphosphorylated tau cannot bind the microtubules (Selkoe 1991; Kar et al. 2002).

NFTs are mostly found in the nerve cells, accumulating mainly in the perikaryon, but following neuron death it can be observed also extracellularly (Selkoe 2001; Duyckaerts et al. 2009). NFTs are particularly abundant in the entorhinal cortex, hippocampus, amygdala, association cortices of the frontal, temporal and parietal lobe and certain subcortical nuclei that project to these regions (Kar et al. 2002; Duyckaerts et al. 2009).

The distribution of NFT-bearing neurons and the severity of neurofibrillary pathology correlate with the intellectual decline gradually developing during the course of AD (Selkoe 1991; Than et al. 2002). The relationship between the tau and amyloid lesions in AD remains elusive (Duyckaerts et al. 2009).

5.1.3 Amyloid-β peptides

In normal individuals, two major forms of Aβ are produced: Aβ1-40 and 1-42. Normally, the majority of the Aβ product is the shorter variety (Kar et al. 2002; Findeis 2007). Aβ1-40 is suggested to have several physiological roles. It works as a cellular antioxydant and secretase inhibitor, and modulates potassium channels in neurons (Findeis 2007). The fibrillarization degree of Aβ1-42 determines its cellular toxicity. The oligomeric Aβ1-42 is far more toxic than the monomeric form, but large insoluble aggregates are less or not toxic (Findeis 2007; Lahiri and Greig 2004; Stephan and Phillips, 2005). Aβ peptides are produced from a precursor protein (amyloid precursor protein, APP), after sequential cleavage by proteases named β- and γ-secretases (Findeis 2007; Stephan and Phillips 2005).

The initial form of amyloid aggregates in the brain is the diffuse plaque. In some regions of the brain, the deposits are only of the diffuse type (presubiculum, striatum, cerebellum and thalamus; Duyckaerts et al. 2009). Diffuse deposits have been found in large numbers in subjects whose intellectual status had been evaluated as normal, leading to the conclusion that these lesions may not be directly toxic (Duyckaerts et al. 2009). Diffuse deposits are associated with apolipoprotein E (ApoE) (Duyckaerts et al. 2009; Selkoe 1991).

The classic senile plaque of AD is a complex lesion of the cortical neuropil containing several abnormal elements. A deposit of extracellular amyloid fibrils forms the core region of the aggregate. This core is surrounded by a high amount of dystrophic neurites (both dendrites and axons), activated microglia and fibrillary astrocytes. These plaques have been reported to contain a wide variety of substances including a number of proteins (like tau protein, lipofuscin and others) in addition to Aβ (Findeis 2007; Selkoe 1991).

The large majority of the Aβ deposits are located in the gray matter, although streaks of diffuse deposits may be seen in the white matter (Duyckaerts et al. 2009). The areal topography of Aβ depositions depends on the stage of the disease and their localization is not random, they follow a distinct sequence (Duyckaerts et al. 2009; Thal et al. 2000). The plaques are formed in the early stage of AD in the medial temporal lobe (MTL: temporal neocortex, entorhinal cortex, hippocampus) and in the cholinerg nuclei (Kar et al. 2004; Thal et al. 2002; Tran et al. 2002). In the later stages of the disease, the depositions are found in the whole neocortex and in several structures of the limbic system (Duyckaerts et al. 2009; Thal et al. 2000). In addition, amyloid deposits – mainly diffuse plaques – occur in the wall of many cerebral and leptomeningeal blood vessels (Duyckaerts et al. 2009). Neuritic (senile) plaques are preferentially found in layers II and III of the neocortex (Selkoe 1991; Duyckaerts et al. 2009).

5.1.4 The amyloid cascade hypothesis

Both genetic and environmental factors can contribute to the development of AD, but the exact mechanism is far to be clear (Kar et al. 2004). Although several theories have been advanced as to the cause and the onset of the disease (Tran et al. 2002), none of them is in accordance with all the clinical and experimental data. A vast amount of data supports the widely accepted amyloid cascade hypothesis (Hardy and Higgins 1992, Hardy 2009). However, the direct link between amyloid deposition and loss of cognitive functions has not yet been proven convincingly (Duyckaerts et al. 2009; Stephan and Philips 2005).

This theory proposes that the main causes of the dementia are the Aβ-related pathological changes observed in the brains of AD patients. The imbalance between Aβ peptide production and clearance initiates a complex, multistep cascade. Briefly, accumulation of aggregated Aβ can be due to different gene defects - missense mutation in the amyloid precursor protein (APP), Presenilin1 (PS1) or Presenilin2 (PS2) genes - or to the presence of the ApolipoproteinE4 allele or other risk factors, altering APP expression, APP proteolytic processing, Aβ stability or Aβ aggregation. The overproduced aggregated amyloid peptide binds to the membrane proteins of the cells and induces Ca^{2+} influx. The high amount of Ca^{2+} disrupts mitochondria, liberating apoptosis inducing factors. Ca^{2+} ions activate protein kinases, initiate hyperphosphorylation of tau protein and formation of neurofibrillary tangles (NFT). These mechanisms induce the collapse of the microtubular system, stop the axonal transport and finally cause cell death (Hardy and Higgins 1992; Hardy and Selkoe 2002;

Selkoe and Podlisny 2002; Stephan and Phillips 2005). The accumulation of amyloid peptide also leads to the appearance of the extracellular amyloid depositions. Around these, neuronal dysfunction, gliosis, inflammatory/neuritic changes, synaptic loss and transmitter loss are observed (Hardy and Selkoe 2002; Dodart and May 2005). This complex pathological process ultimately leads to Alzheimer's disease.

The main goal of our study was to establish a good and relatively simple AD model in rats using administration of human Aβ1-42 into the medial temporal lobe or bypassing the BBB via intranasal delivery.

5.2 Neurobiology of the medial temporal lobe

The medial temporal lobe is a system of anatomically related structures that are essential for declarative memory. The system consists of the hippocampal region (CA fields, dentate gyrus (DG) and subicular complex), and the perirhinal, entorhinal and parahippocampal cortices (Forwood et al. 2005; Squire et al. 2004).

5.2.1 Anatomical organization of the hippocampus

The hippocampal region is formed by two sheets of cells folded into interlocking Cs.

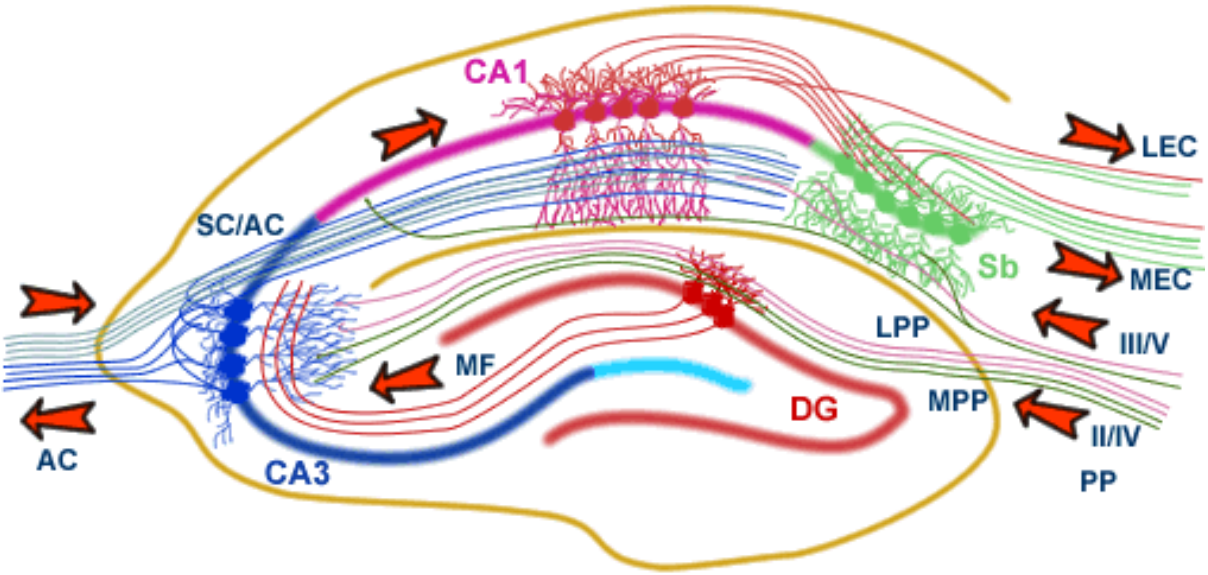

Fig. 1. A composite illustration of the rat hippocampal formation, with input and output projections. The hippocampus forms a principally uni-directional network, with input from the EC that forms connections with DG and CA3 pyramidal neurons via the perforant pathway (PP). CA3 neurons also receive input from the DG via mossy fibres (MF) and send axons to the CA1 via Schaffer collaterals (SC), as well as to contralateral CA1 via the Association Commissural pathway (AC) (http://www.bristol.ac.uk/synaptic/info/pathway/hippocampal.htm; Siegel and Sapru 2006).

The outer C is the Cornu Ammonis (or Ammon's horn) that can be divided into CA1, CA2 and CA3; the inner C is the DG (Fig. 1.). The subicular complex is the most inferior component of this formation; it lies between the hippocampus proper and the EC (Shapiro 2001).

Two major parts of the hippocampus are the CA3 and CA1 (Fig. 1.). Excitatory input to CA1 pyramidal neurons is extensive. About 5000 CA3 pyramidal cell axons – comprising the Schaffer collateral pathway – converge on a single CA1 cell. These Schaffer collaterals form synapses at all levels of the CA1 cell's dendritic tree – close to the cell body and farther. CA3 axons make contact with the dendrites of many other CA1 pyramidal cells mainly on dendritic spines (Fig. 1., Kandel et al. 2000).

In many parts of the brain, spines have two inputs, one excitatory and the other inhibitory. In area CA1, however, each pyramidal cell spine of hippocampus has only one synapse, which is excitatory. These spines may function as separate biochemical regions because the neck of the spine restricts diffusion between the head of the spine and the rest of the dendrite (Shapiro 2001; Kandel et al. 2000; Bhatt et al. 2009).

The hippocampus is a recipient of convergent projections from adjacent cortical structures – located earlier in the hierarchy of information processing – and projects also back to the higher order cortical areas. The cortical axons make synapses on cells in the DG, which in turn innervate the CA and these return input to the cortex (Broadbent et al. 2004, Squire et al. 2004; Seward and Seward 2003).

5.2.2 Anatomical organization of the entorhinal cortex

The EC harbors different subdivisions, which specifically mediate the connectivity with functionally different sets of cortical and subcortical areas in the brain. Brodmann divided the entorhinal cortex field into two areas - a lateral and a medial region - on the basis of cytoarchitectonic criteria. These areas also respond to and thus convey different types of information: cells in the medial subdivision are spatially modulated, whereas cells in the lateral EC most likely convey olfactory and somatosensory information. All regions of the EC project to all parts of the hippocampus (Canto et al. 2008; Seward and Seward 2003).

Similarly to other cortical areas, the EC has also a vertical partition. The lamination of the EC generally is considered the prototype of the transition between the three-layered allocortex and the six-layered neocortex. There is massive reciprocal connectivity between deep and superficial layers of the EC (Fig. 2., Canto et al. 2008; Heinemann et al. 2000).The

EC has complex intrinsic and network properties that contribute to signal processing. The reciprocal synaptic connectivity between deep and superficial layers of the EC leads to massive excitation largely driven by N-methyl-D-aspartate (NMDA) receptors (Heinemann et al. 2000).

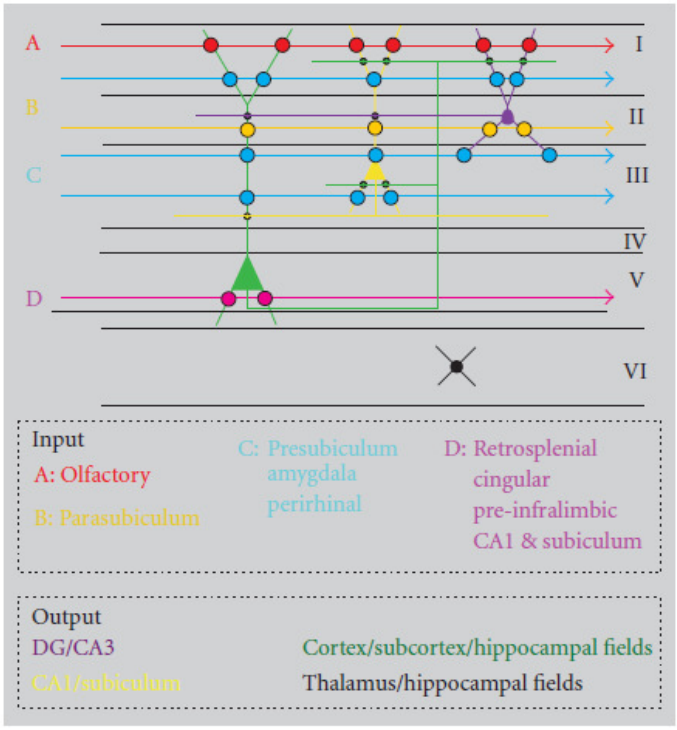

Fig. 2. Schematic representation of laminar distribution (arrows) and synaptic interactions (circle) between inputs and principal cells of the entorhinal cortex. Circles indicate putative synaptic contacts between inputs and principle cells. Main output connectivity of principle cells is indicated as well. (Canto et al. 2008).

5.2.3 Connectivity between the hippocampus and entorhinal cortex

The EC conveys multimodal processed information from the sensory cortical areas to the hippocampus, as well as information from the HC processed through the EC to permanent storage sites in the neocortex (Heinemann et al. 2000; Poucet et al. 2003). The EC also has extensive cortical and subcortical connections, in particular with the basal forebrain, claustrum, amygdala, basal ganglia, thalamus, hypothalamus, brainstem in addition to the MTL (Fig. 2., Canto et al. 2008; Sewards and Seward 2003).

The EC is a major input and output structure of the hippocampal formation relaying information from and to the neocortex (Fig. 2.; Kopniczky et al. 2006; Canto et al. 2008). Between the entorhinal cortex and the hippocampus there are multiple and reciprocal connections. Projections to the hippocampus are derived from specific layers of EC (Canto et al. 2008; Heinemann et al. 2000). The EC provides major inputs to the hippocampal formation through the perforant pathway. The stellate cells of layer II give rise to projections

that distribute to the dentate gyrus (DG) and CA3, while pyramidal cells of layer III terminate on neurons in CA1 and subiculum. A small number of deep layer (IV–VI) neurons of the EC also project to the DG and hippocampus.

The dentate gyrus and the CA3 field of the hippocampus do not project back to the EC. Thus, the recipients of the layer II projection do not have any direct influence over the activities of the EC. It is only after the layer II and layer III projection systems are combined in CA1 and subiculum that return projections to the EC are generated. The return projections mainly terminate in deep layers of EC and they are exactly in register (i.e. they are point-in-point reciprocal) with the entorhinal inputs to these areas. Thus, at the global level, all of the circuity is available for reverberatory circuits to be established through the loop, starting and ending at the EC. This confirms the critical role of the EC with respect to the input and output from the hippocampus (Canto et al. 2008; Seward and Seward 2003; Heinemann et al. 2000). The strong connections of the hippocampus and the EC have important roles in memory processes (Heinemann et al. 2000; Poucet et al. 2003).

5.2.4 The role of the medial temporal lobe in the memory process

Different types of memory processes involve different regions and combinations of regions in the brain (Fig. 3.).

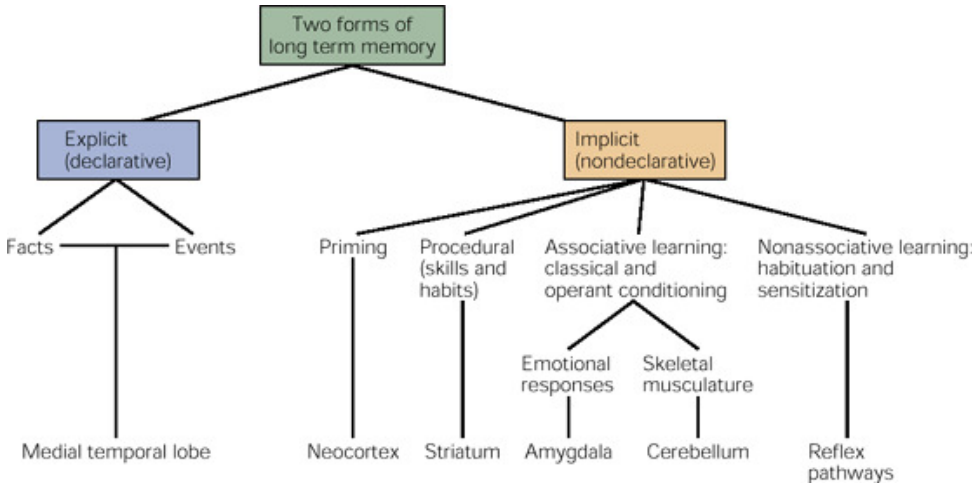

Fig. 3. Classification of different memory types with the brain areas that mainly responsible for them. There are two fundamental forms of memory: implicit or nondeclarative memory and explicit or declarative memory. Explicit memory can be further classified as episodic (a memory for events and experience) or semantic (a memory for facts; Kandel et al. 2000).

Explicit memory underlies the learning of facts and experiences – knowledge that is flexible can be recalled by conscious effort and can be reported verbally (Forwood et al. 2005). Implicit memory processes include forms of perceptual and motor memory –

knowledge that is stimulus-bound, is expressed in the performance of tasks without conscious effort, and is not easily expressed verbally. It flows automatically in the doing of things, while explicit memory must be retrieved deliberately (Kandel et al. 2000; Squire et al. 2004).

The structures of the MTL constitute one of the convergent zones of cortical processing and receive input from all the sensory modalities (Squire et al., 2004). Declarative memory is stored in the MTL for some time and is eventually transferred to other brain regions (mainly to the cerebral cortex) for permanent storage, a process called system consolidation (Frankland and Bontempi 2005, Thomson and Kim 1996; Forwood et al. 2005). MTL has a specific role in associative or recollective aspects of declarative memory and mediates the initial steps of long-term storage (Kandel et al. 2000, Squire et al. 2004).

The hippocampus is the critical component of the region in memory processes (Forwood et al. 2005, Kandel et al. 2000). HC projects place or contextual information to the neocortex, which rebound with object representations to form complex, multimodal memories in the hippocampus (Broadbent et al. 2004, Forwood et al. 2005, Kandel et al. 2000). The hippocampus lies at the end of a cortical processing hierarchy and the entorhinal cortex is the major source of its cortical projections, therefore the impairment of EC accompanies cognitive dysfunction (Broadbent et al. 2004). EC has an important role in different types of learning, in the formation of spatial and recognition memory and some forms of operant learning (Squire et al. 2004; Seward and Seward 2003; Kopniczky et al. 2006; Parron et al. 2004).

5.3 Olfactory system

5.3.1 Anatomical and physiological characteristics of the olfactory system

The olfactory system is a relatively simple, highly conserved structure across vertebrate evolution and has long been implicated as having unique ties to memorial processes (Wilson et al. 2008).

This region has very strong anatomical ties to the limbic system including the amygdala and the hippocampus, strong interconnections with the perirhinal and entorhinal cortex, and projects also to the higher-order cortex (e.g., orbitofrontal cortex, olfactory cortex). The olfactory system is heavily innervated by well-defined neuromodulatory systems known to be important for memory and neural plasticity (Wilson and Linser 2008).

5.3.2 The olfactory system is a unique gate of the CNS to bypass the BBB

Olfactory sensory neurons are the only first order neurons whose cell bodies are located in the distal epithelium. Their dendritic processes are directly exposed to the external environment in the upper nasal passage while their unmyelinated axons, constituting fila olfactoria, project through perforations in the cribriform plate of the ethmoid bone to synaptic glomeruli in the olfactory bulb. In the bulb, the axons synapse with mitral cell dendrites forming the glomeruli and project to limbic system, hippocampal formation and higher-order cortex (Fig. 4.). These unique anatomical and physiological properties of the olfactory region provide both extracellular and intracellular pathways into the central nervous system (CNS) that bypass the blood-brain-barrier (BBB) (Illum 2000; Thorne et al. 2004).

Following nasal administration, a large number of low molecular weight drugs and peptides, such as estradiol, progesterone, cocaine or cholecystokinin have been shown to reach the cerebospinal fluid (CSF), the olfactory bulb and in some cases other parts of the brain, such as the frontal cortex and the hippocampus (Van den Berg et al. 2004, Thorne et al. 2004). Even large molecules, such as the protein insulin-like growth factor and fibroblast growth factor could be transported to the CNS (Thorne et al. 2004; Wang et al. 2008).

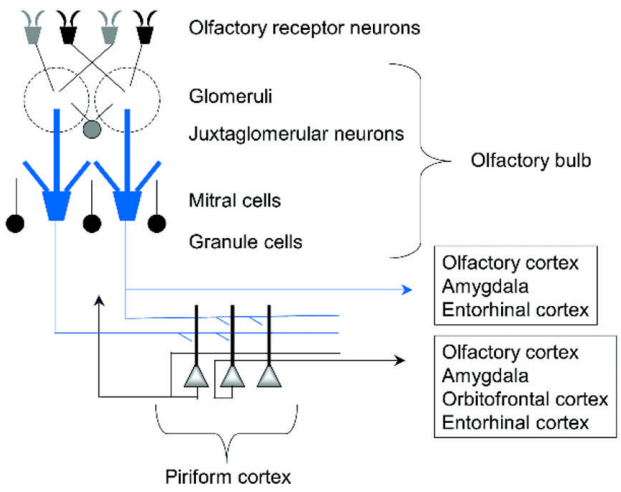

Fig. 4. Schematic representation of mammalian olfactory system circuitry: connections of the olfactory bulb with higher-order structures (Wilson et al. 2004).

5.4 In vivo models of amyloid pathology

5.4.1 Transgenic models

Gene targeting has become a popular technique to study the action of proteins in the otherwise intact nervous system. Selective inactivation of the genes (knock out) allows one to study the functional chain from gene to behavior by investigating the effects of the genetic lesion at the cellular and behavioral level including learning and memory (Wolfer et al. 1998).

There are several transgenic mouse lines that carry mutant genes and develop progressive, age-related Aβ neuropathology, especially in the HC and neocortex (Puolivali et al. 2002). Mutations in the genes linked to familiar AD, such as those encoding the amyloid precursor protein (APP) or presenilin-1 (PS-1) proteins, result in increased brain levels of Aβ. Recently, the senescence-accelerated mouse prone/8 (SAMP8, a murine model for accelerated secescence), showing age-related deficits in learning and memory, has been used in Alzheimer research (Banks et al. 2003).

By altering APP metabolism, elevated brain levels of Aβ can be observed from the age of 6-12 months. Parallel to the appearance Aβ depositions, there is a substantial increase in astrocytes and microglia. Cognitive deficit is observed after these histopathological changes, at the age of about 9-16 months (Arendash et al. 2001; Puolivali et al. 2002). A very recent publication of Morrissette et al. (2009) provides a detailed summary of the relevance of transgenic mouse models to human AD.

5.4.2 Non-transgenic models

5.4.2.1 Spontaneous and injection models

Several mammalian species, but not rodents, spontaneously develop diseases resembling AD: old monkeys and bears develop plaques and tangles, and plaques have been seen in old dogs, cats, and in mouse lemurs (reviewed in Duyckaerts et al. 2009). However, these species have a number of practical disadvantages such as housing costs, long life-spans etc.

Several studies have investigated the effects of Aβ injection into the rodent brain. Most infusion models have been developed under the assumption that Aβ deposition in the

brain is a requisite to inducing behavioral impairments and that acute Aβ injection to brain induces learning and memory impairment (Dodart and May 2005).

In these models, the nature and degree of cognitive impairments observed after Aβ injection depend largely on the targeted structure, the Aβ sequence length and aggregation state, the solvent, the time elapsed after the injection and the behavioral tasks used (Chacon et al. 2004; De Ferrari et al. 2003; Shen et al. 2001; Stephan and Phillips 2005). The peptides are mainly injected into the MTL, cholinerg nuclei or cerebral ventricles (Chacon et al. 2004; Casamenti et al. 1998). Injection to the MTL is of interest because this area is important for mammalian memory, and damage to this region impairs performance in various tasks of learning and memory in a way similar to AD (Broadbent et al. 2004). Another interesting region is the basal forebrain, as loss of cholinergic nerve cells within this structure and depletion of several markers of the cholinerg system (ChAT and AChE) are typical in AD (Dodart and May 2005). Studying the effect of intracerebroventricular infusion of synthetic human Aβ peptide in normal rodents evolved from the idea that producing elevated levels of Aβ in the brain would be conducive to pathological events, and neurodegeneration of the limbic area could cause behavioral deficit related dementia (Stephen and Philips 2005).

An important advantage of Aβ injection methods compared to transgenic technology is that they offer the possibility to test the effects of different forms of Aβ in different brain structures, and thus to shed light on the importance of these factors in the pathomechanism of AD. It has been shown, for instance, that injection of soluble (monomeric or oligomeric) forms of Aβ induces an immediate, but transient impairment of memory because of their detrimental effects on synaptic plasticity (Cleary et al. 2005; Stephan and Phillips 2005). On the other hand, injections of aggregated insoluble forms of Aβ (or of the soluble but highly fibrillogenic Aβ1-42) lead to later-onset and longer-lasting effects on memory, related probably to inflammatory reactions induced by fibrillar Aβ (Stephan et al. 2003; Stephan and Phillips 2005).

5.4.2.2 New perspective: nasal pathway to the CNS

Among the models of AD, exogenous drug or peptide administration into the brain is still the most cost-effective method that is widely used. These methods are time-consuming and may induce tissue lesions, however the less invasive systemic targeting of these compounds to the central CNS is difficult to fulfill because of the BBB (Pardridge 2005). Several approaches have been attempted in order to enhance the blood to brain transport and

deliver drugs to the brain in an effective concentration. These methods include (i) the manipulation of BBB: hyperosmotic shock, vasoactive substances, inhibition of efflux transporters (Deli 2009); (ii) the modification of the molecules: lipophilic or cationic changes, prodrugs, binding of drugs to carriers, e.g. transferrin (Pardridge 2005). However, the increased transport of drugs to the CNS can be carried out not only by the modification of the BBB functions or the drug molecule itself, but also via an (iii) alternative route by selection of an application site circumventing the BBB, like the nasal pathway (Illum 2000; Thorne et al. 2004). It is important to keep in mind that the BBB participates in the pathomechanism and contributes to the progression of AD, and regulates the brain levels of Aβ by efflux transporters (Iadecola 2003; Zlokovic 2005).

Intranasal administration of drugs offers a potential route to the CNS and avoidance of hepatic first-pass elimination, because olfactory sensory neurons possess unique anatomic and physiologic features (Introduction 5.3; Illum 2000; Wilson 2008; Wolburg et al. 2008). These special neurons extend their projections from the external environment to the olfactory bulb bypassing the BBB (Thorne et al. 2004; Wolburg et al. 2008). Intranasal delivery of drugs offers several advantageous properties. This method is non-invasive and essentially painless. Furthermore, it ensures rapid absorption, the avoidance of first-pass metabolism in gut and liver and does not require sterile preparations (Zhang et al. 2004).

5.5 Aims

The main aim of our work was to establish and validate an AD model in rats, showing cognitive impairments due to brain damage. We tried to develop two models of Aβ pathology for answering the following questions:

1) Concerning the first model (administration of human Aβ1-42 into the rat entorhinal cortex):

    1. What are the effects of Aβ1-42 injection to the EC on behavior? Does it induce cognitive deficits similar to those observed in AD?

    2. What are the histopathological effects of the protofibrillar-fibrillar form of human Aβ1-42 injected into the EC of rats? Are they similar to neuropathological signs of AD?

3. On the basis of these results, can protofibrillar-fibrillar Aβ1-42 injection into the EC of rats be used as an appropriate model of AD?

2) Concerning the second model (intranasal administration of human Aβ1-42):

1. Can Aβ1-42 be targeted into the CNS by intranasal administration in rats? Which parts of the brain does it reach? What are the histopathological effects of intranasal Aβ1-42 administration?

2. What are the effects of intranasal Aβ1-42 on behavior? Does it induce cognitive deficits similar to those observed in AD?

3. On the basis of these results, can intranasal Aβ1-42 administration in rats be used as an appropriate model of AD?

6 MATERIALS AND METHODS

6.1 Subjects and housing

Adult male Wistar rats (Harlan, Hungary, bred at the University facility), weighing 300-350g at the beginning of the experiment were used as subjects. After arrival in the laboratory, they were housed by groups of four under constant temperature and lighting conditions (23°C, 12:12 h light/dark cycle, lights on at 07:00). Rat chow and tap water were provided *ad libitum*. All efforts were made to minimize animal suffering throughout the experiments. Experiments were performed in accordance with the Hungarian Health Committee and the European Communities Council Directive of 24. November 1986 (86/609/EEC). Formal approvals to conduct the experiments have been obtained from the Animal Experimentation Committees of the University of Szeged and of the Biological Research Center, and from the local authorities (XVI./03835/001/2006).

6.2 Peptides and nasal formulations

Human Aβ1-42 was synthesized in our laboratory as it was previously described (Zarandi et al. 2007). Aβ1-42 peptide was labeled with 7-amino-4-methyl-3-coumarinylacetic acid (AMCA) at the N-terminus using Fmoc strategy resulting in a very stable covalent binding of the dye to the peptide (Zarandi et al. 2007). Both the Aβ1-42 and the AMCA-Aβ1-42 batches contained oligomers, protofibrils and fibrils according to quasielastic light scattering, atomic force and transmission electron microscopy measurements (Hetényi et al. 2008). All reagents were purchased from Sigma-Aldrich (Budapest, Hungary), unless otherwise indicated.

During the intranasal experiment, a special mucoadhesive vehicle was used. The composition of this dosing solution was as follows: 10% w/w polyoxyl 40 hydrogenated castor oil (Cremophor RH40; BASF, Germany), 5% w/w hydroxypropyl cellulose (Klucel EF; Hercules Inc., Wilmington, DE, USA), 50% diethyleneglycol monoethyl ether (Transcutol HP; Gattefossé, St-Priest, France). In order to ensure the complete dissolution of the polymer, samples were rehomogenized after 24 h. Then 1 mg/ml Aβ1-42 or AMCA-Aβ1-42 peptides were dissolved in Transcutol HP and mixed with the solution containing Cremophor RH40 and Transcutol HP in a ratio of 1 to 1 to ensure both dissolution of peptide

and mucoadhesivity. Aβ1-42 solutions were always prepared freshly before nasal administration and were used within 1 h after dissolution.

6.3 Administration of Aβ1-42

6.3.1 Aβ1-42 injection into the EC ("entorhinal model")

Rats (n=54) were anaesthetized by intraperitoneal injection with a mixture of ketamine (10.0 mg/100g) and xylasine (0.8 mg/100g). They were then placed in a stereotaxic frame, a midline sagittal incision was made in the scalp, and holes were drilled on the skull. The solution was injected into the EC at three bilateral sites (2.5µl per site) with a Hamilton syringe in a total of 60 minutes. The coordinates were (from bregma): AP: -6.4, -6.8, -7.8; ML: ±4.0, ±3.6, ±3.0; DV: -8.2, -7.8, -7.4 (Paxinos and Watson, 1982). Control animals (CONTROL group) were injected with sterile physiological saline. Amyloid-treated rats (AMY group) were injected with a 10^{-4} M Aβ1-42 solution in distilled water prepared immediately before injection. It has been shown that this solution contains mostly protofibrillar and fibrillar form of Aβ1-42 (Zarandi et al. 2006). NMDA-treated rats (NMDA group) were injected with a 0.04 M NMDA solution in distilled water.

6.3.2 Intranasal administration procedure ("intranasal model")

Nasal administration was performed as follows. Rats (n=44) were anaesthetized intraperitoneally with tribromoethanol (10 ml/kg body weight). The tribromoethanol solution (1.25 w/v %, pH 7.0) was previously filtered (with 0.45 µm sterile syringe filters) and stored for maximum one week in dark sterile bottles at 4 °C. Anaesthetized rats were placed in supine position. The experimental solution was then administered by a micropipette positioned 5 mm deep into the right naris to achieve the longest possible residency time of the vehicle in the nasal cavity (Horvát et al. 2009). AMCA-Aβ1-42 was administered as a single dose of 10 µg/40 µl into the right naris of 4 rats. Other animals received 12.5 µg/25 µl unlabeled Aβ1-42 or vehicle as a repeated dose (experiment 1: once daily for 28 days; experiment 2: twice daily for 7 days) into both nasal cavities. Control animals received the same amounts of vehicle.

6.4 Experimental schedules

6.4.1 Entorhinal model

In this study, Aβ1-42 solution, NMDA or vehicle was injected into the EC of rats' brains. The animals (9 intact, 17 control, 18 amyloid-treated, 10 NMDA-treated rats) were allowed to recover for 10 days before the beginning of the behavioral tests. The experimental protocol is schematically represented on Fig. 5.

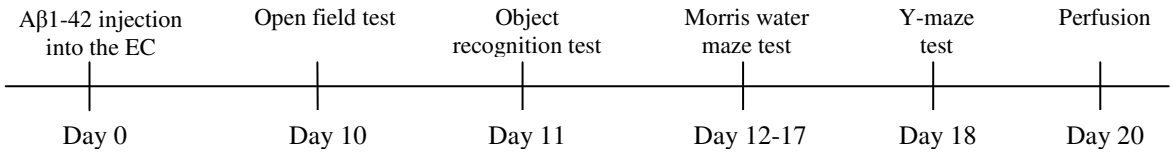

Fig. 5. Schematic representation of the experimental schedule of the entorhinal Aβ1-42 model.

6.4.2 Intranasal model

6.4.2.1 AMCA-Aβ1-42 administration

AMCA-Aβ1-42 was administered intranasally in order to observe its distribution in the brain. Brain samples were taken after transcardial perfusion at a delay of two hours for fluorescent microscopy (n=4), and at 30, 60, 120, 180, 240 and 480 min delays for spectroscopy (n=5x2), as shown on Fig. 6.

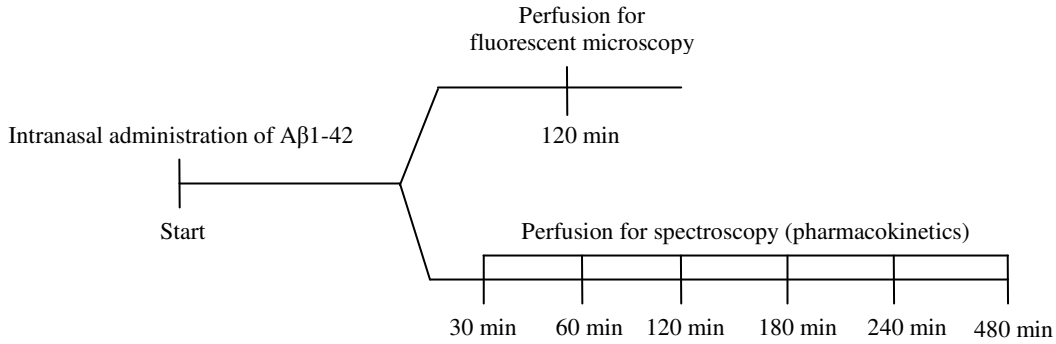

Fig. 6. Schematic representation of the schedule of the intranasal AMCA-Aβ1-42 experiment.

6.4.2.2 Aβ1–42 administration

The behavioral experiments were carried out with different administration protocols (Fig. 7.). In Experiment 1, Aβ1-42 solution or vehicle was administered nasally once a day in

the morning (n=10 rats in each group) for 28 days. In the second study (3 experimental groups: intact (non-treated and non-anaesthetized), vehicle or Aβ1-42-treated, n=12 rats in each), rats were administered with vehicle or peptide nasally twice daily (morning and afternoon) for 7 days. Behavioral experiments were performed two days after the last administration of Aβ1-42 and any anaesthetics.

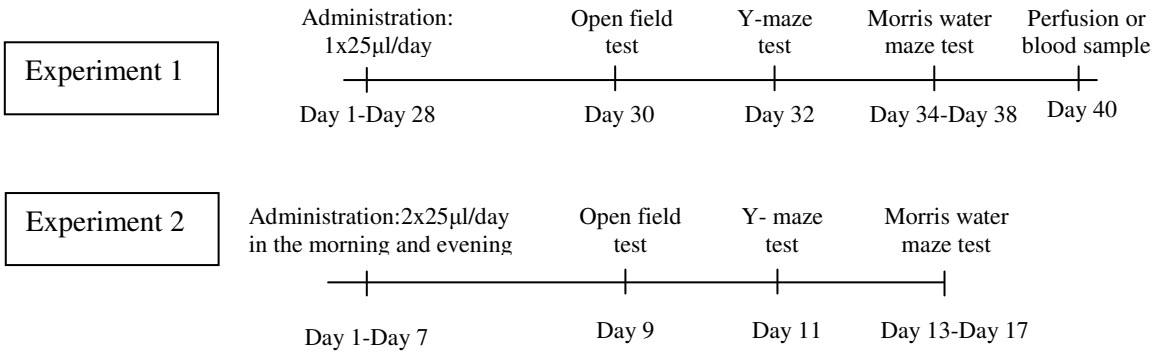

Fig. 7. Schematic representation of the experimental schedule of intranasal Aβ1-42 model.

6.5 Behavioral testing

Rats were handled and weighed each day after the operation. All the behavioral experiments were carried out in the same room, illuminated by a halogen lamp giving diffused and dim light. A video camera was mounted on the ceiling directly above the test apparatus and relied to a video tracking system. The behavior of the animals was automatically and/or manually recorded with the software EthoVision 2.3 (Noldus Information Technology, Netherlands, 2002).

6.5.1 Open field test

Open field test was performed in order to assess the consequences of Aβ1-42 administration on explorative behavior and anxiety. The open field consisted of a black plastic rectangular arena (50x70x30 cm), the floor of which was covered with wood chips. At the beginning of the test, the animals were placed in the centre of the arena, and left to explore it freely for 5 minutes. The following parameters were determined automatically: (1) total traveled distance, (2) percent time spent in the peripheral zone (thigmotaxis, Simon et al. 1994). The behavior was also scored by an observer who was unaware of the treatment of individual rats to record rearing, grooming and defecation behaviors.

6.5.2 Object recognition test

The object recognition test was used to assess whether recognition memory is impaired by Aβ1-42 treatment. This test was carried out in the open field apparatus, on the day following the open field test, which therefore served also as a habituation session to the environment of the object recognition test. The test consisted of a single acquisition session (sampling phase), followed by a retention test 2 h later. Two types of objects were used, different in color, shape and material. For acquisition, each rat was placed in the middle of the arena containing two identical objects, and was left to explore them freely for a total of 30 seconds of object exploration. Exploration of an object was defined as directing the nose to the object at a distance of less than 2 cm or touching it with the nose. Turning around or sitting on the object was not considered as object exploration. The animal was then placed back in the home cage for 2 hours. Object recognition was tested in a 5-minute session, during which one object used during the acquisition phase was replaced by a novel object.

The nature and the spatial position of the objects were counterbalanced within each group in order to avoid any bias due to a preference that rats may have for a given object or its position in the arena. During the retention phase, the duration of exploration of each object was recorded, and the ratio of novel object exploration / total exploration was expressed as a percentage.

6.5.3 Spatial navigation in the Morris water maze

Spatial learning and memory were assessed in a Morris water maze. The maze consisted of a circular tank made of blue plastic (diameter: 130 cm, height: 80 cm) filled to a depth of 45 cm with water of 21±1°C. The water was rendered opaque by the addition of milk. The tank was divided into four virtual quadrants. A white, hidden escape platform (diameter: 10 cm) was submerged in the middle of one of the quadrants (training quadrant), 30 cm from the rim of the pool and 2 cm below the water surface. The platform was not visible at water level. The rats had to learn to find the hidden platform on the basis of several constant spatial cues around the pool.

For the entorhinal model, the training phase consisted of five blocks of three trials. They were conducted between 9:00 and 13:00 (on days 1, 2 and 3 of the test), and between 14:00 and 18:00 (on days 1 and 2 of the test). For the intranasal model (Experiment 1 and 2), the training phase consisted of five blocks of four trials conducted on successive days between 9:00 and 13:00.

Four different starting positions were used at the limits of the quadrants around the perimeter of the tank. A trial began by placing the rat into the water facing the wall of the pool; the starting position was varied pseudo-randomly over the trials. Rats were given a maximum of 90 s to find the platform and were then allowed to stay on it for 10 s. If a rat failed to escape from the water within 90 s, it was gently guided to the platform, and stayed there for 10 s. After the acquisition phase, retention was assessed in a 60-s probe trial (trial with the platform removed), on the day following the last training block. During acquisition trials, the time to reach the platform (latency), swim path lengths (distance) and swim speed was recorded. During the probe test, percent time spent in each of the 4 virtual quadrants and the number of crossings over the platform's original position were measured. The means of the data from each block of trials were used for statistics.

6.5.4 Spontaneous alternation in a Y-maze

Y-maze test was carried out in order to assess short-term memory. The apparatus was made of wood painted in black, and had three identical arms (each 14 cm wide, 19 cm high and 51 cm long), positioned in an equal angle. The floor of the maze was covered by wood chips. At the beginning of the test, each rat was placed in the centre of the arena facing one arm. During the 10-min test period, the animal was allowed to move freely throughout the maze. The sequence of arm entries was recorded manually. Spontaneous alternation behavior was defined as successive entries into the three arms, on overlapping triplet sets (Yamada et al. 1998). Percent spontaneous alternation behavior was calculated as the ratio of actual to possible alternations, the latter defined as (total number of arm entries – 2).

6.6 Statistics

The results of different groups in the open field, object recognition, water-maze probe test and Y-maze tests were compared with one-way analysis of variance, followed by Fisher's LSD post-hoc tests for multiple comparison when appropriate. In the Morris water maze test of entorhinal model, the swimming latency and distance data in entorhinal model did not have a normal distribution, they were therefore analyzed with the nonparametric Kruskal-Wallis test, followed by Mann-Whitney U-tests for multiple comparison. The distribution of date was normal in Morris water maze test of intranazal model and there was used one-way ANOVA for analysis. Mean performance for individual groups was compared to chance level by one-

sample Student's t-test. The exploration durations of the two objects during the acquisition phase, as well as the time spent in the target and other quadrants in the Morris water maze were compared by paired Student's t-test. All data presented are means ± S.D. Statistical significance was set at $p<0.05$. Statistical analysis was done with GraphPad Prism software (GraphPad Software Inc., San Diego, CA, USA) or SPSS statistics program.

6.7 Histology

6.7.1 Tissue preparation

After the behavioral tests, rats were killed by transcardial perfusion. They were deeply anaesthetized and perfused through the ascending aorta with 100 ml phosphate buffered saline solution (PBS; room temperature, pH 7.4), followed by 300 ml of ice cold paraformaldehyde solution (4% in phosphate buffer, pH 7.4). The brains were removed, postfixed in the same fixative for 2 h, cryoprotected in sucrose solution (30% in PBS) for at least 36 hours at +4°C, and cut on a cryostat in 30 µm coronal sections. Brain slices were collected and stored at +4°C in PBS for free-floating immunohistochemistry or thioflavin-T staining.

AMCA-Aβ1-42 injected rats were transcardially perfused two hours after the operation. Their brains were removed, cut in blocks and frozen in liquid nitrogen, then embedded in Tissue-Tech OCT (PS002; Sakura, Tokyo, Japan) compound. Blocks were stored frozen at - 80 ºC until cutting with cryostat. Thirty-µm thick sagittal sections were collected on glass slides, air dried and mounted in Gel Mount (Biomeda, USA).

6.7.2 Immunohistochemistry and Thioflavin-T staining

Glial fibrillary acidic protein (GFAP) immunoreactivity (IR) – indicating reactive astrocytosis – was visualized by immunostaining with rabbit antibody (DakoCytomation, Glostrup, Denmark) used at a 1:20000 dilution in PBS (pH 7.4). Aβ1-42 was equally visualized by immunohistochemistry using a mouse monoclonal antibody (4G8; AbCam Cambridge, UK) used at a 1:500 dilution. At least six sections per brain (every twelfth section) from the dorsal hippocampus to the EC, from 9 control and 9 amyloid-treated rats were immunostained. The sections were processed at the same time and using the same solutions to reduce variability in immunostaining. After quenching of endogenous peroxidase

activity and a blocking step, the sections were incubated overnight at 4°C with the primary antibody in the presence of 20% goat serum and 0.2% Triton X-100. On the following day, the sections were washed in PBS and incubated 1 h at room temperature with the secondary biotinylated mouse anti-rabbit antibody for GFAP (1:400) and goat anti-mouse for 4G8 (Vector Labs, 1:500). The peroxidase reaction was carried out using the Vectastain Elite ABC Kit system (Vector Labs, Burlingame, California, US) using diaminobenzidine as the substrate and $NiCl_2$ as an intensifier. After immunostaining and washing, all sections were mounted on gelatin-coated slides, air-dried, dehydrated and coverslipped with DPX mountant for histology (Fluka BioChemika Buchs, Switzerland). For fibrillar amyloid-specific thioflavin-T staining (e.g. Kayed and Glabe 2006), brain slices were mounted on gelatin-coated slides and dried overnight at room temperature. They were then washed in distilled water, incubated with a 0.5% thioflavin-T (Sigma-Aldrich, St. Louis, Missouri, US) solution for 30 min, dehydrated and coverslipped.

6.7.3 Microscopy and analysis

The fluorescent signal of brain sections from AMCA-Aβ1-42 or thioflavin-T injected rats was examined by a Nikon Eclipse TE2000 fluorescent microscope (Nikon, Japan) and photographed by a Spot RT digital camera (Diagnostic Instruments, USA). Digital photographs after immunohistochemistry were taken using a light microscope (Olympus Vanox-T AH-2) and a CCD camera (Spot RT, Diagnostic Instruments).

The observer of the sections was unaware of the treatment of the brains during the qualitative analysis, which was done with a computerized image analysis system (ImagePro Plus, Media Cybernetics, U.S.A.).

6.8 Measurement of peptide concentration by spectroscopy

For pharmacokinetics experiments brains were collected at 30, 60, 120, 240 and 480 min after a single nasal treatment (Fig. 6.: a single dose of 10 µg/40 µl of AMCA-Aβ1-42; n=4/group). To determine the concentration of AMCA-Aβ1-42 at different time points after the administration, deeply anaesthetized animals were cardially perfused with 50 ml saline, brains were removed and dissected to the following regions: right and left olfactory bulb, right and left frontal and parietal cortex, hippocampus, midbrain, cerebellum and pons. Samples

were homogenized with 2 ml of PBS in Potter–Elvehjem tissue grinders. Homogenized samples were sonicated for 2 minutes while cooling with ice cold water bath. Six ml of methanol for liquid chromatography (LiChrosolv, Merck Chemicals, Darmstadt, Germany) was added to the samples under stirring. Samples were then centrifuged at 50000 g for 10 min at 4°C. The AMCA-Aβ1-42 content of the supernatants was determined by a PTI spectrofluorometer (Photon Technology International Inc., South Brunswick, NJ, USA) at an excitation wavelength of 345 nm and an emission wavelength of 445 nm. The sensitivity of the measurement was 1 ng/ml AMCA- Aβ1-42 in the samples. Linearity of the measurement of AMCA- Aβ1-42 was $r^2 \geq 0.985$, while the precision was found to be RSD $\leq 9.08\%$ across all the concentration ranges used in the study.

6.9 Anti-human Aβ1-42 titer measurement by ELISA

Blood samples were collected from vehicle- or Aβ1-42-treated rats of behavior Experiment 1 at the end of the treatment period (n=6 rats in each group) to determine anti-human Aβ1-42 immunotiter by enzyme-linked immunoabsorbent assay (ELISA). Maxisorp ELISA multiwell plates (Thermo Fischer Scientific, Waltham, MA, USA) were coated with 1.25, 2.5 or 5 μg/ml Aβ1-42 in 50 mM sodium carbonate buffer pH 9.6 overnight at 4°C and rinsed three times with Tris-buffered saline (TBS, 25 mM Tris, 150 mM NaCl, 2 mM KCl, pH 7.4) containing 0.05% bovine serum albumin (v/w). Microtiter wells were treated with blocking buffer (1% bovine serum albumin and 5% goat serum in 0.05%TBS) pH 7.4 for 2 h in room temperature and the diluted serum samples from the rats (dilutions: 10-1000) were added to the microtiter wells. As a positive control mouse anti-human Aβ1-42 monoclonal antibody (4G8, AbCam, Cambridge, UK) was used (dilutions: 4000 to 16000). The plates were incubated with biotin-conjugated anti-mouse IgG and IgM antibody (Jackson ImmunoResearch Laboratories, Inc., West Grove, PA, USA; 1:10000), then with extravidin peroxidase (1:2000), both at room temperature for 30 min. We determined in a separate experiment that the antibody reacts with rat immunoglobulins. After washing, plates were incubated with phenylene-diamine (0.33 mg/ml in citrate buffer; pH: 6.0) for 10 min and the reaction was stopped by the addition of 2 M H_2SO_4. Optical density was determined at 450 nm using a Multiscan Ascent plate reader (Thermo Fisher Scientific Inc., Waltham, MA, USA).

7 RESULTS

In this chapter, the results of our two models will be represented separately: first, the results of the entorhinal model, then those of the intranasal model.

7.1 Entorhinal model

7.1.1 Behavior

7.1.1.1 Open field

In the open field test, parameters of exploratory behavior (total distance traveled, rearings) and anxiety (% time spent on periphery, grooming, defecation) were measured 10 days after the injections. Results showed that there was no significant difference among the groups in any of these parameters (total distance traveled: $F_{3,50}$=0.14, p=0.93; rearings: $F_{3,50}$=0.93, p=0.43; % time spent on periphery: $F_{3,50}$=1.73, p=0.17; grooming: $F_{3,50}$=0.13, p=0.94; defecation: $F_{3,50}$=2.13, p=0.11).

7.1.1.2 Object recognition memory

The object recognition task was conducted on the day following the open field test, in the same apparatus. The two objects were explored equally during the acquisition phase (t=0.28, p=0.78).

During the retention phase, significant between-group differences in performance were observed ($F_{3,50}$=4.41, p=0.007). Specifically, both intact and control rats explored preferentially the novel object (time spent exploring the novel object significantly different from chance level; t_{18}= 4.72, p=0.0001 and t_8=3.04, p=0.01, respectively; Fig. 8), while rats injected with Aβ1-42 or with NMDA showed a similar level of exploration of the novel and familiar objects (t_{17}=1.06, p=0.3 and t_9=0.78, p=0.45, respectively; Fig. 8). Between-group comparisons showed that intact and control rats had similar recognition memory performance and performed better than the Aβ1-42-treated or NMDA-treated rats (AMY-control: p=0.009; AMY-intact: p=0.006; NMDA-control: p=0.038; NMDA-intact: p=0.02). All the groups had a similar overall duration of object exploration during the retention phase ($F_{3,50}$=0.98, p=0.43).

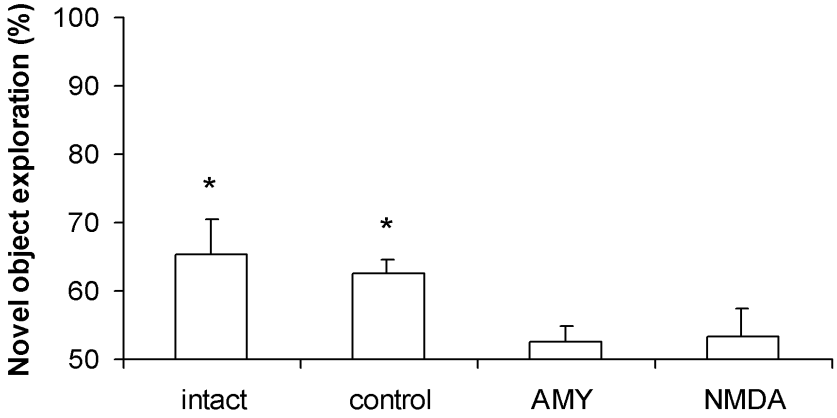

Fig. 8. Aβ1-42 or NMDA injection into the entorhinal cortex impairs object recognition memory. Retention performance is expressed as the percent time spent exploring the novel object over the total time of object exploration (mean ± SEM). Intact and control animals explored preferentially the novel object while performance of animals injected with Aβ1-42 (AMY) or NMDA did not differ from chance level. *different from chance level at $p<0.05$.

7.1.1.3 Spatial learning and memory in the Morris water maze

The Morris water maze test was used to assess spatial learning and memory on days 12-16 after the injections. The results showed that although performance of each group improved significantly across blocks of trials, learning was slower in the Aβ1-42- and the NMDA-treated groups, compared with control rats (Fig. 9.A). Specifically, in the third block, Aβ1-42- and NMDA-treated rats swam longer distances to find the platform than control rats ($H_{3,31}=7.63$, $p=0.05$; control-AMY: $p=0.027$, control-NMDA: $p=0.1$). In the fourth block, intact rats were quicker to find the platform than all the other groups ($H_{3,31}=10.57$, $p=0.01$; intact-control: $p=0.02$; intact-AMY: $p=0.007$; intact- NMDA: $p=0.006$). No differences were observed between NMDA and Aβ1-42-treated groups in the third or the fourth block ($p=0.847$ and $p=0.700$, respectively). There were no significant differences among the groups during the other blocks (first block: $H_{3,31}=3.3$, $p=0.34$; second block: $H_{3,31}=4.18$, $p=0.24$; fifth block: $H_{3,31}=6.86$, $p=0.07$). Despite slower learning in the Aβ1-42-treated and NMDA-treated rats, performance at the probe test given 24 hour after learning showed that spatial memory was not impaired in this task (Fig. 9.B). All groups spent more time in the training quadrant than in the others (compared to the mean of the time spent in the other quadrants; intact $t_7=5.88$, $p=0.001$; control $t_8=3.31$, $p=0.01$; AMY $t_7=10.4$, $p<0.001$; NMDA $t_8=4.80$, $p=0.001$). The four groups spent a similar amount of time in the training quadrant ($F_{3,31}=0.29$, $p=0.83$). Finally, there were no significant differences in swim speed among the groups at any stage of behavioral testing.

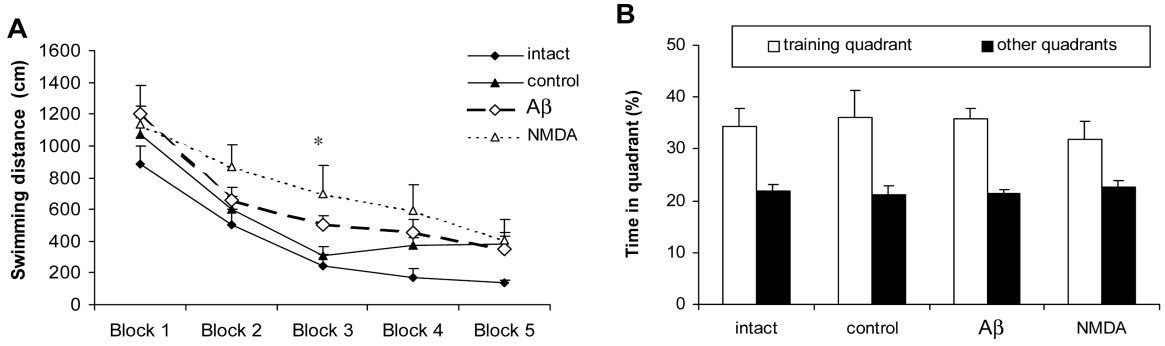

Fig. 9. Injection of Aβ1-42 or NMDA in the entorhinal cortex resulted in slower spatial learning in the water-maze. (A) Performance during acquisition is expressed as the mean (± SEM) swim paths lengths (distance) during the 5 training blocks. In block 3, AMY and NMDA rats swam a longer distance than controls to find the platform. By block 5, however, there was no significant difference between groups. (B) Injection of Aβ1-42 or NMDA did not affect performance in the probe trial 24 h after training. All groups spent more time in the training quadrant than in the other 3 quadrants, with no significant difference between groups (mean ± SEM are shown) (mean ± SEM are shown).

7.1.1.4 Spontaneous alternation in Y-maze

The effect of Aβ1-42 on spontaneous alternation was examined on day 17 post-injection in a Y-maze. All groups showed alternation performance above chance level (50%, intact: t_8=3.27, p=0.011; control: t_{18}=6.79, p<0.0001; AMY: t_{17}=7.17, p<0.0001; NMDA: t_9=5.63, p=0.0003; Fig. 10.). The performance of the groups did not differ from each other ($F_{3,50}$=0.058, p=0.98). Moreover, the total number of arm entries was comparable in the different groups ($F_{3,50}$=1.95, p=0.13), suggesting a similar level of motivation for exploration (Fig. 10.).

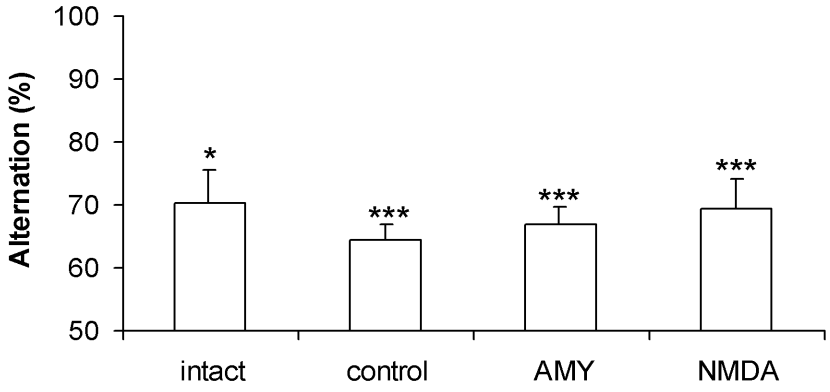

Fig. 10. Injection of Aβ1-42 or NMDA did not alter spontaneous alternation behaviour in a Y-maze. Histograms show the percent alternation (consecutive entries into 3 different arms) over the total number of arm entries for each group (mean ± SEM). * p<0.05; *** p<0.001, compared to chance.

7.1.2 Histology

After behavioral testing, three weeks after Aβ1-42 injections, histological examination was performed on the brains of amyloid-treated and control rats to assess inflammatory reaction and the presence of aggregated material in the entorhinal cortex.

7.1.2.1 GFAP-immunohistochemistry

GFAP staining was used to detect reactive astrogliosis as an indication of an inflammatory reaction. In contrast to control animals in which slight astrogliosis was found restricted to the injection tracts (Fig. 11.A, C), likely caused by mechanical damage, astrocyte proliferation was apparent in a much larger area extending further apart from the amyloid injection sites in the entorhinal cortex (Fig. 11.B, D). Moreover, in amyloid-treated animals, astrocyte somata had a larger appearance and GFAP staining was more intense than in controls.

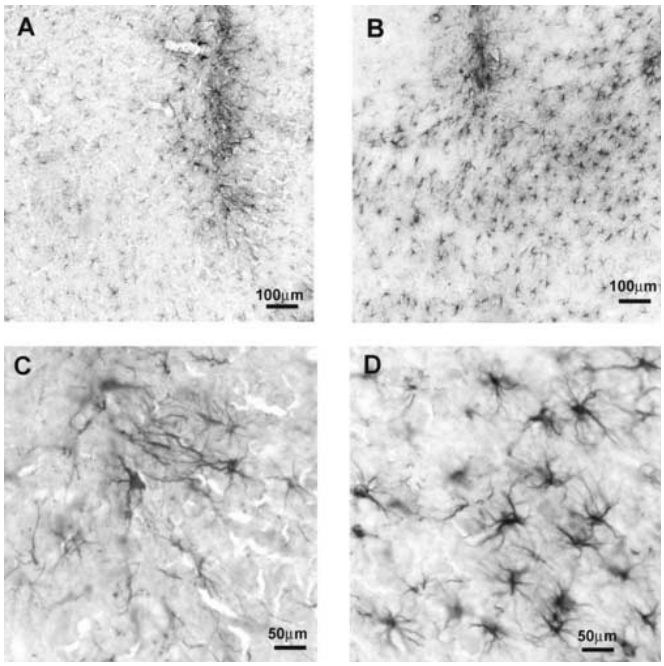

Fig. 11. Representative examples of GFAP staining in the entorhinal cortex of a control (A, high magnification: C) and an Aβ1-42-injected (B, high magnification: D) rat. In control animals, only some reactive astrocytes along the injection tract can be observed among normal glial elements. In the amyloid-treated group, numerous reactive astrocytes can be seen around the injection sites, extending to the whole entorhinal cortex.

7.1.2.2 Amyloidβ1-42 staining

Specific amyloid immunostaining (4G8) and thioflavin-T positive staining was used to assess whether injection of Aβ1-42 peptides lead to amyloid deposits in the entorhinal cortex. Examination of the EC revealed plaque-like depositions in Aβ1-42-injected animals (Fig. 12.B, C), but only non-specific staining in controls (Fig. 12.A). The presence of amyloid depositions was the highest around the injection sites, with only a few deposits observed in

other parts of EC. The diffuse plaque-like structures were diverse in size, but they were all composed of many fibril-like structures.

The presence of fibrillar Aβ1-42 was confirmed by the strong thioflavin-T positive staining observed in the EC (Fig. 12.D), as this colorant is specific for Aβ of fibrillar structure (Kayed and Glabe, 2006).

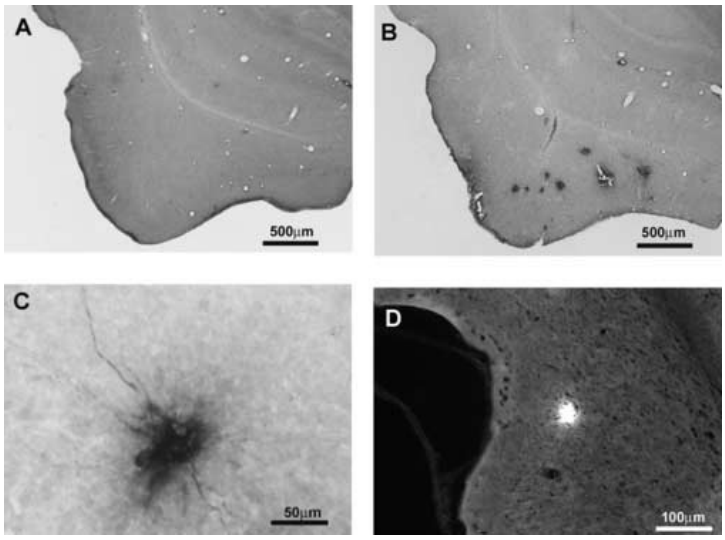

Fig. 12. Representative examples of sections showing Aβ1-42 staining (4G8 antibody) in the entorhinal cortex of a control (A) and an amyloid-injected (B, C) rat. In the amyloid-treated group, aggregates with apparent filaments can be seen around the injection sites (B, high magnification: C). The fibrillar nature of at least some amyloid aggregates is confirmed by positive thioflavin-T staining (light patch on D).

7.2 Intranasal model

At the beginning of this intranasal study, the regional penetration of the peptide was studied with AMCA-Aβ1-42 administration was started after the exact determination of peptide distribution in the rat brain. Two different administration protocols of Aβ1-42 were used (Fig. 7.). The second protocol was shorter than the first, with less frequent anaesthesia, but the concentration and the volume of the peptide was unchanged.

7.2.1 Intranasal AMCA-Aβ1-42 administration

7.2.1.1 Fluorescent microscopy

AMCA-Aβ1-42 could be detected by fluorescent microscope two hours after nasal administration (single dose) in the dorsoanterior region of the olfactory bulb and in the frontal

cortex of rats (Fig. 13.A-D), anatomically close to the site of administration. Using the same imaging parameters, no fluorescence could be seen in the same brain regions of vehicle treated animals (Fig. 13.A, 13.C). Increased blue fluorescence intensity indicating the penetration of the peptide, as compared to vehicle-treated rats, was also seen in distant brain regions, like pons and cerebellum. Diffuse staining shown on Fig. 13.B, 13.D is typical after nasal treatment and 2 hours time-frame. A similar staining pattern can be seen when fluorescently labeled dextran is administered nasally to rats (Horvát et al. 2009).

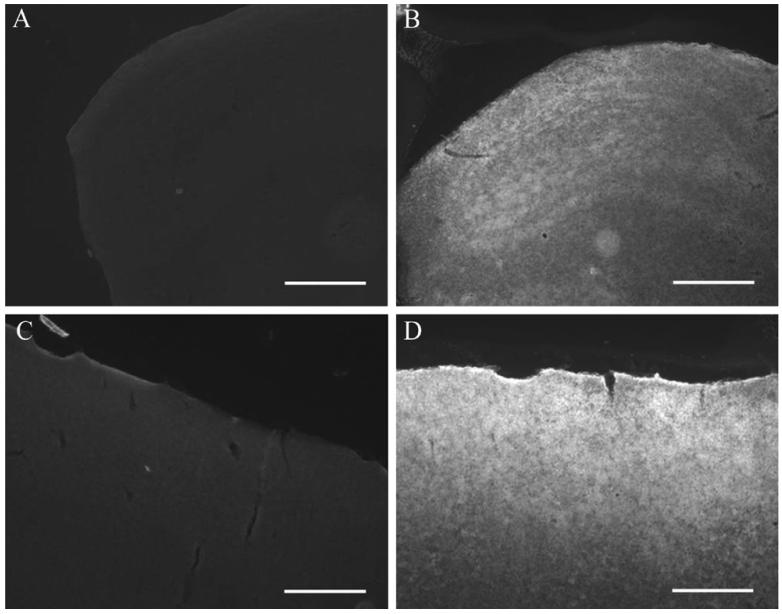

Fig. 13. Representative fluorescent microscopy images of unfixed, frozen sections from the olfactory bulb and the frontal cortex from rats treated with vehicle (control; A, C) or Aβ1–42 labeled with blue fluorescent dye amino-methyl coumarin (AMCA-Aβ1–42) for 2 h (B, D). Fluorescence was detected only in AMCA-Aβ1–42 treated rats (B, D).

7.2.1.2 Spectroscopy

The penetration of nasally administered AMCA-Aβ1-42 to different brain regions was quantified at different time points by spectroscopy (Fig. 14.A). In this kinetic study the highest concentration of AMCA-Aβ1-42 was found at 120 min after a single intranasal administration of the peptide (Fig. 14.A-B). Besides olfactory bulbs, different amounts of the labeled peptide were measured in samples from cortical regions, hippocampus, midbrain, cerebellum and pons (Fig. 14.B), showing a similar distribution pattern as found by Thorne et al. for nasally administered insulin-like growth factor-I (Thorne et al. 2004).

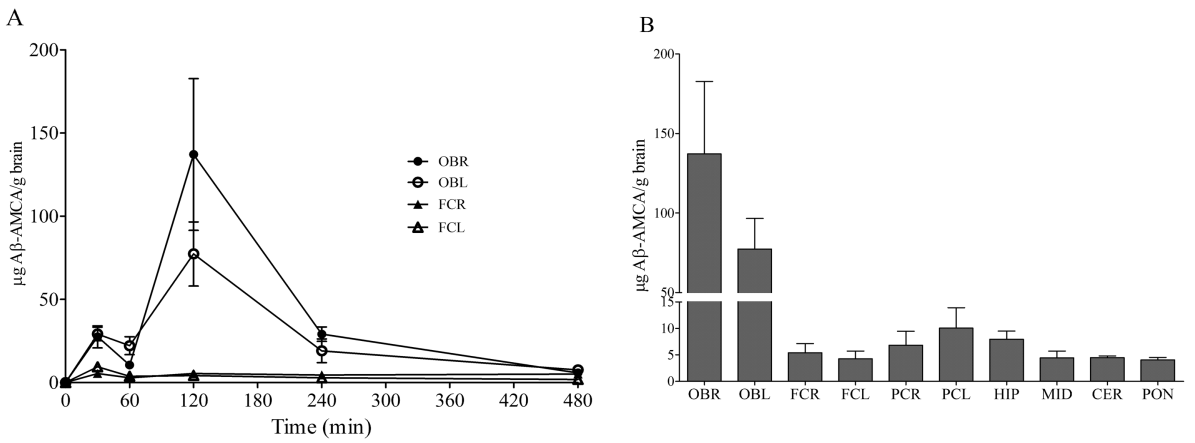

Fig. 14. A: Kinetics of brain concentrations of AMCA-Aβ1–42 in four brain regions, right and left olfactory bulb, right and left frontal cortex samples of rats after intranasal administration of the peptide (mean ± SD, n=4). B: AMCA-Aβ1–42 concentrations in different brain regions measured 120 minutes after intranasal administration of the peptide (mean ± SD, n=4). (OBR: right olfactory bulb; OBL: left olfactory bulb; FCR: right frontal cortex; FCL: left frontal cortex; PCR: right parietal cortex; PCL: left parietal cortex; HIP: hippocampus; MID: midbrain; CER: cerebellum; PON: pons).

7.2.2 Intranasal Aβ1-42 administration

7.2.2.1 Behavior

7.2.2.1.1 Open field test

In the open field test, % time spent on periphery (thigmotaxis) was measured as an index of anxiety. Results showed that Aβ1-42 treatment did not affect this parameter (Exp1: t_{18}=0.30, P=0.77; Exp2: $F_{2,22}$=0.41, P=0.67).

7.2.2.1.2 Morris water maze test

The Morris water maze test was used to assess spatial learning and reference memory after Aβ1-42 administration (Fig. 15.A, 15.B). The performance of each group improved significantly across days in both experiments, however, learning was slower in the Aβ1-42-treated rats compared with control and intact animals (Fig. 15.B).

In Experiment 1, there were no significant differences between groups on any day (day 1: t_{18}=0.48, P=0.64; day 3: t_{18}=1.13, P=0.27; day 4: t_{18}=1.18, P=0.25; day 5: t_{18}=0.2, P=0.84), although on the second day, control rats were quicker to find the platform (but this effect failed to reach statistical significance: t_{18}=2, P=0.06).

In Experiment 2, one-way ANOVA revealed a difference among groups on the second and third days (day 2: $F_{2,22}$=4.44, P=0.02; intact versus Aβ1-42: P=0.06, control versus Aβ1-42: P=0.04, and control versus intact: P=1.00, day 3: $F_{2,22}$=4.04, P=0.03, intact versus Aβ1-42: P=0.07, control versus Aβ1-42 P= 0.06, and control versus intact P=1.00). No differences were observed among groups on the first, fourth and fifth days (day 1: $F_{2,22}$=0.63, P= 0.54; day 4: $F_{2,22}$=3.07, P=0.06; day 5: $F_{2,22}$=0.96, P= 0.39).

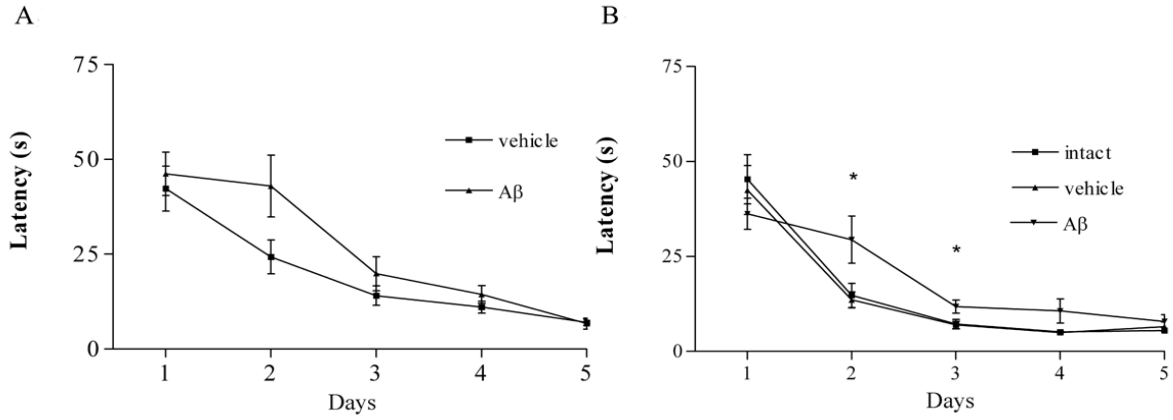

Fig. 15. Behavioral results from two different treatment schedules with nasal administration of Aβ1–42 to rats (Exp1: A, Exp2: B). A, B: Performance of vehicle-treated (control), Aβ1–42–treated and intact rats in the Morris water maze in the first and second experiment, respectively. Histograms show the escape latency during the reference memory testing period (mean ± SD, n=8-9/ treatment group, *P<0.05 compared with control groups).

7.2.2.1.3 Y-maze test

In the Y-maze, short term memory was assessed by calculating spontaneous alternation rate (Fig. 16.A and 16.C). In both experiments, all groups showed alternation performance above 50% chance level (Exp1: control: t_5=4.69, p=0.005; Aβ1-42: t_6=3.56 p=0.01; Exp2: intact: t_8=6.09 p<0.0001; control: t_7=9.27 p<0.0001; Aβ1-42: t_7=7.29 p<0.0001). The performance of the groups did not differ from each other (Exp1: t_{11}=0.16, p=0.87; Exp2: $F_{2,22}$=0.76, P= 0.45). Moreover, the total number of arm entries did not differ among the different groups of rats, indicating that changes in alternation behavior were not due to generalized exploratory, locomotory or motivational effects (Exp1: t_{11}=0.71, p=0.49; Exp2: $F_{2,22}$=1.29, P= 0.29).

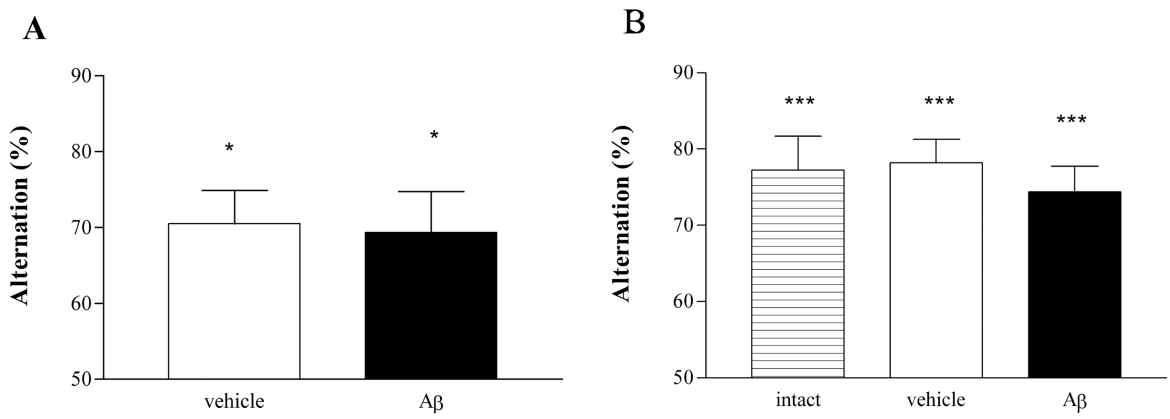

Fig. 16. Behavioral results from two different treatment schedules with nasal administration of Aβ1–42 to rats (Exp1: A, Exp2: B). Performance of vehicle-treated (control) or Aβ1–42–treated and intact, non-treated and non-anesthetized, rats in a Y-maze in the first and second experiment, respectively. Histograms show the percentage of spontaneous alternation (consecutive entries into three different arms) over the total number of arm entries for each group (mean ± SD, n=6-10/treatment group).

7.2.2.2 Aβ1-42 immunohistochemistry

Immunohistological examination was performed on the brain of rats treated nasally by vehicle or Aβ1-42 to detect the presence of Aβ1-42 in different regions, such as the olfactory bulb, the frontal cortex and the hippocampus.

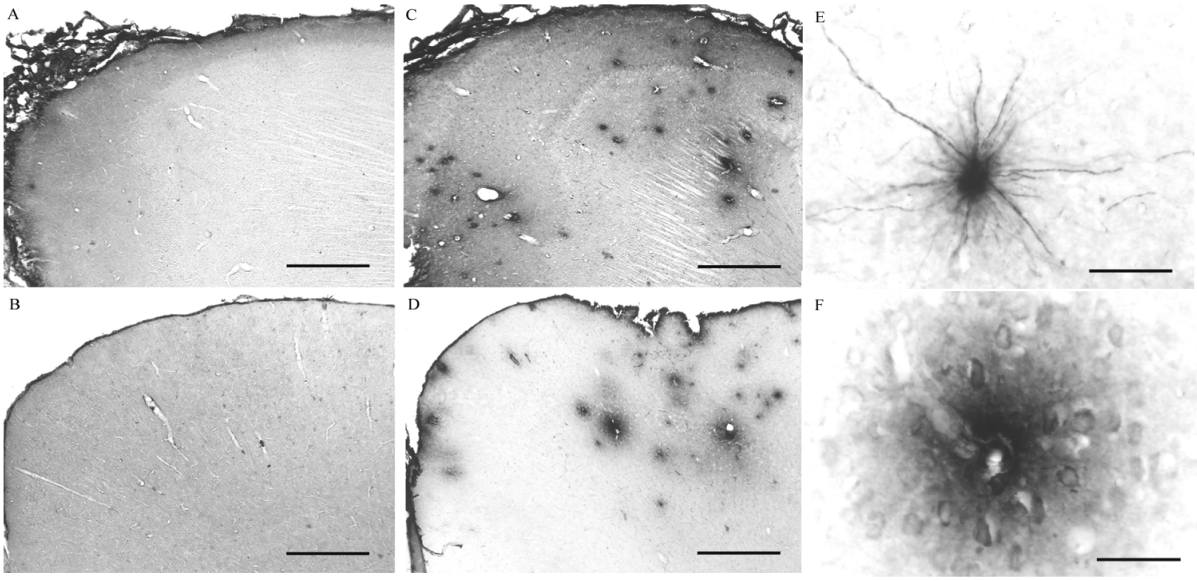

Fig. 17. Representative examples of sections showing immunohistochemical staining for Aβ1–42 using 4G8 antibody in the olfactory bulb and frontal cortex from rats treated with vehicle (control; A, B) or Aβ1–42 for 28 days (C-F). In the amyloid-treated group, immunopositive deposits and diffuse staining pattern around blood vessels (F) can be seen. Scale bar: 500 µm (A-D), 50 µm (E-F).

Immunostaining revealed plaque-like depositions in all these regions of Aβ1-42 treated animals (Fig. 17.C, D), while no plaques were found in rats receiving vehicle only (Fig. 17.A, B). The presence of amyloid immunostaining was the highest in the olfactory bulb (Fig. 17.C), in agreement with the AMCA-Aβ1-42 data.

7.2.2.3 ELISA test

To rule out a vaccination effect, the anti-Aβ1-42 immunoglobulin titers were checked in the serum of rats treated nasally with Aβ1-42 for 28 days. No anti-Aβ1-42 immunoglobulin titer, exceeding the nonspecific background, could be detected by a sensitive ELISA method in sera (dilution: 1:10-1:1000; Fig. 18.). In contrast, 4G8 antibody gives a high reading at much higher dilutions (1:4000-1:16000; Fig. 18.).

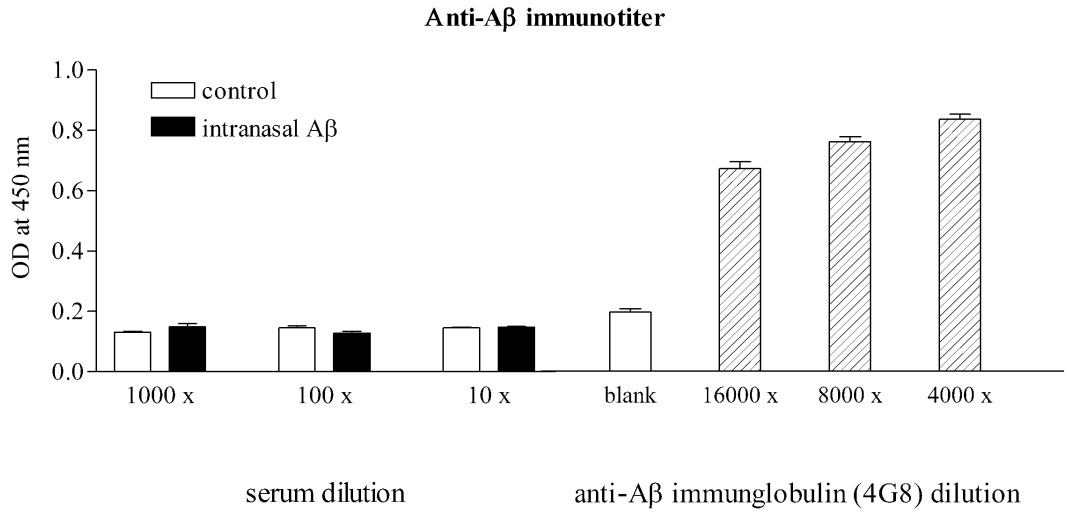

Fig. 18. A sensitive ELISA was used to determine the concentration of anti-human Aβ1–42 antibodies present in the sera of nasally treated rats for 28 days. As a positive control, 4G8 anti-human Aβ1–42 antibody was tested. No anti-Aβ1–42 immunotiter could be detected from rat sera by ELISA. Blank: background reading of wells without primary antibody.

8 DISCUSSION

A huge body of research on AD shares the common purpose of understanding the molecular pathogenic pathway of AD controlling behavioral and neurological symptoms, in order to delay the progression of the disease, and ultimately to prevent its onset. A relevant animal model is necessary for understanding disease pathogenesis correlates between certain types of lesions and behavior. An animal model that reproduces the complexity of the pathogenic mechanisms and most of the clinical symptoms of AD still represents a challenge, but a useful model should recapitulate at least a part of the neuropathology and cognitive impairment (Dodart and May 2005).

The main aim of the present study was to establish and validate an AD model in rats, showing cognitive impairments due to brain damage. For this purpose, two models of Aβ pathology were developed and the cognitive and morphological effects of administered human Aβ1-42 were observed.

Currently, two types of AD models are widely used: transgenic animals and injection models. Spontaneous models are also very interesting, but the housing cost of these larger species is prohibitive for most laboratories, and the behavioral tests for studying their cognitive functions are less well known than the standard rodent tests.

The transgenic models are more specific for the human AD, but the cost of the transgene technology limits their applicability. Another disadvantage of this type of model is that they remodel primarily the familiar form of AD, which represents only a small proportion of the cases (Findeis et al. 2007, Wolfer et al. 1998). Moreover, in these models several compensatory mechanisms can mask the expected deficit (Wolfer et al. 1998).

Different rodent injection models reproduce several characteristics of AD such as amyloid deposition, neurofibrillary tangles, lesions, neurotoxicity, or behavioral symptoms (Dodart and May 2005). In most experiences, a suitable form of the amyloid peptide is injected into a specific brain region (Chacon et al. 2004; Seabrook et al. 2004). However, other exogenous chemicals may be systemically administered (Nivsarkar et al. 2008), or neurons linked to AD, like those of the cholinergic system, can be specifically lesioned (Nag and Tang 1998) in order to reproduce lesions, neurotoxicity, or behavioral symptoms observed in AD.

The models targeting amyloid peptide to the brain are particularly valuable tools for studying AD-related memory deficits. On the one hand, they provide important data for

understanding the pathomechanism of neurotoxicity, and on the other hand, they can be used for testing new therapeutic strategies and drug candidates for AD (Dodart and May 2005; Chacon et al. 2004; Juhász et al. 2009, Stephan and Philips 2005).

8.1 Entorhinal model

The purpose of the first part of our work – protofibrillar-fibrillar Aβ1-42 injection into the entorhinal cortex – was to examine the specific contribution of amyloid pathology in the EC to the cognitive deficits associated with AD, and thereby to assess whether this type of injection can be used as a model for AD. To this end, we investigated the histopathological effects of Aβ1-42 injection into the EC, and tested learning and memory abilities of injected rats in different tasks believed to depend on the integrity of medial temporal lobe structures.

8.1.1 Histopathological effects of protofibrillar-fibrillar human Aβ1-42 injection into the EC

Our histological analysis showed that the injected soluble Aβ aggregated into plaque-like structures in the EC. We also confirmed previous data showing signs of intense inflammatory reaction characterized by activation of astrocytes and microglial cells surrounding and infiltrating the deposits formed after the injection of aggregated Aβ, regardless of the target structure in the CNS (Stephan and Phillips 2005). Accumulation of astrocytes has also been observed around senile plaques in human AD, and their peripheral distribution around Aβ deposits suggests a role in containing or circumscribing the abnormal protein, a well-known function of astrocytes in response to injury (Vehmas et al. 2003). Moreover, a recent study in a triple transgenic mouse model of AD reported that the inflammatory reaction that occurs in this model appears earlier in the EC than in the hippocampus (Janelsins et al. 2005). Although we cannot dissociate the specific contribution of aggregated amyloid peptide and inflammation in the memory deficits observed here after injection in the EC, it is possible that cognitive dysfunction induced by fibrillar Aβ into the EC can be at least in part due to the associated extensive inflammatory reaction (Stephan et al. 2003; reviewed in Sastre et al. 2006).

8.1.2 Behavioral effects of Aβ1-42 injection into the EC

Our results showed for the first time that injection of Aβ into the EC of rats results in selective impairments in memory functions, characterized by spatial learning retardation and severe deficits in object recognition memory.

Recognition memory is dependent on the integrity of structures of the medial temporal lobe, including the hippocampus and possibly to an even greater extent, the surrounding parahippocampal areas (see review in Mumby 2001; Squire et al. 2004). Previous studies have shown that excitotoxic lesions of the EC impair recognition memory in rats (Galani et al. 1998; Mumby and Pinel 1994; Parron and Save 2004). Here, we confirm the importance of the EC in object recognition memory, as NMDA injections severely impair performance in the novel object recognition task, and we show that injection of Aβ1-42 also results in a similar recognition memory deficit in this task. The deficit cannot be accounted for by an alteration in object exploration, as all rats explored the two novel objects for an identical time during the acquisition phase and had a similar amount of total object exploration during the test phase.

Spatial reference memory measured in the Morris water maze is largely dependent on an intact hippocampus, and can also be affected by lesions of certain parahippocampal areas (reviewed in Aggleton et al., 2000). EC lesions have been reported to impair place navigation (Aggleton et al. 2000; Kopniczky et al. 2006; Parron et al. 2004; Spowart-Manning and van der Staay 2005). However, some studies failed to find an effect of EC lesions (e.g. Galani et al. 1998), probably due to the use of proximal rather than distal landmarks (Parron et al. 2004), or to other differences in experimental paradigms affecting the choice of different navigational strategies in the water maze (Aggleton et al. 2000). In our experimental conditions, NMDA lesion of the EC slowed down the rate of spatial learning, without otherwise affecting the rat's ability to learn with repeated training or the expression of good spatial memory performance 24h after training. With injections of Aβ1-42, again a similar profile of impairment was observed.

In our experimental conditions we found no evidence for working memory impairment in the spontaneous alternation task after either NMDA or Aβ1-42 injection. Although there is some evidence that the EC may be involved in this task, at least at some point of ontogeny (Blozovski and Hess 1989; Degroot and Parent 2000), spatial working memory deficits are more consistently found after hippocampal lesions (reviewed in Lalonde 2002) and,

interestingly, working memory deficits have been clearly identified after Aβ1-42 injection into the hippocampus (Stephan et al. 2003).

8.1.3 Applicability of entorhinal injection of protofibrillar-fibrillar human Aβ1-42 in rats as an appropriate model of AD

Taken together, our results reveal that injection of Aβ1-42 inducing the formation of stable Aβ aggregates in the EC results in a profile of cognitive impairments similar to that observed after NMDA injection, suggesting that Aβ induces functional alteration of the EC. Bilateral excitotoxic lesion of the EC in rats has been suggested as a model for the early stages of human AD, because they share some similarities in their pathological and cognitive characteristics (Spowart-Manning and van der Staay 2005). Moreover, cholinergic drugs used in the treatment of AD have been reported to improve recovery from the behavioral deficit induced by EC lesion (Spowart-Manning and van der Staay 2005). However, injection of excitotoxic molecules is likely to induce neuron loss or lesions in the EC that have a neuropathological origin different from the lesions observed in AD. Our model therefore seems more suitable in the context of understanding the etiology of AD or for testing therapeutic candidate molecules designed to protect against Aβ pathology.

In conclusion, our results suggest that injection of protofibrillar-fibrillar Aβ1-42 into the EC of rats constitutes a suitable experimental model for several aspects of the early stages of AD. This *in vivo* model could be valuable for investigating specifically in the EC the differential pathological and cognitive consequences of different sequences and different aggregation states of Aβ peptides, and for screening drug candidates designed to combat the deleterious effects of protofibrillar-fibrillar Aβ.

8.2 Intranasal model

Injecting synthetic Aβ1-42 consisting of oligomers, protofibrils, and fibrils similar to the Aβ1-42 samples used in our entorhinal model (and other studies) into the hippocampus, the EC or the cholinergic nuclei exerts deleterious effects on learned behavior in rats (Chacon et al. 2004; Casamenti et al. 1998). These infusion methods work well for many aspects of AD research as mentioned previously, however, these procedures have several drawbacks: they are acute, need long and invasive surgery using a stereotaxic frame, moreover, the injected volume is very limited, therefore the effects of chronic administration or large

amounts of peptides cannot be studied. Chronic administration of Aβ1-42 to brain areas can be also achieved by osmotic pumps (Nitta et al. 1994), but it is not widely used because of its cost, the frequent obstruction of the pump by Aβ1-42 aggregates, and high mortality due to infectious and inflammatory reactions.

For the above mentioned reasons, the second part of our work focused on developing a new method of Aβ administration, which is non-invasive, cheap and easy to apply: the intranasal route.

8.2.1 Penetration of intranasally administered Aβ1-42 into the CNS

The nasal pathway represents a new route to the CNS for peptides or proteins bypassing the BBB (Banks et al. 2003; Illum 2004; Thorne et al. 2004). Nose to brain delivery was demonstrated for vasopressin, insulin and nerve growth factor in both animal and human studies (Illum et al. 2004). Intranasally delivered insulin-like growth factor-I can bypass the BBB via olfactory- and trigeminal-associated extracellular pathways to rapidly elicit biological effects at multiple sites within the brain and spinal cord, and in agreement with our findings, it was detected in the olfactory bulbs and rostral brain regions, like frontal cortex (Thorne et al. 2004). Several factors, especially mucoadhesive and absorption enhancing agents, can increase the nasal absorption of molecules or drugs. It has been recently demonstrated that a nasal vehicle containing both mucoadhesive and absorption enhancing components increased the transport of 4 kDa FITC-dextran, the size of Aβ1-42 peptide, from the nasal cavity to several brain regions, including olfactory bulb, frontal cortex, hippocampus, midbrain and pons (Horvát et al. 2009), similarly to our present results.

We demonstrated by fluorescent microscopy, spectroscopy and immunohistochemistry that Aβ1-42 can be delivered to the CNS – in particular, to the olfactory bulb, the frontal cortex and the hippocampus – after nasal administration of the peptide. Moreover, immunohistochemistry revealed that in all the regions reached by Aβ1-42, plaque-like depositions were formed in treated animals.

The nasal administration of Aβ1-42 is widely used in vaccination studies, where the goal of the injection is the immunization of the animals for developing an experimental therapy of AD (Seabrook et al. 2004). It is important to note that our goal was entirely different from these works. Repeated monthly injections of Aβ1-42 dissolved in immune adjuvants lead to an antibody response associated with a remarkable clearance of Aβ1-42

deposits (Hartman et al. 2005). In our case, Aβ peptide was dissolved in a special nasal formulation increasing brain penetration (Horvát et al. 2009) that could have elicit immune activation. We thus took special precautions: the length of administration did not exceed 28 days, and we omitted adjuvants leading to immunostimulation. A sensitive ELISA test could not detectable no anti-human Aβ1-42 immunotiter, therefore our protocol did not elicit immune activation.

Our results are in agreement with recent findings showing effective brain delivery of different drugs and peptides after intranasal administration (Illum 2000; Banks et al. 2003; Thorne et al. 2004). To our knowledge this is the first study to show that administration of Aβ1-42 via the nasal route can represent an easy, simple brain targeting method for this bioactive peptide.

8.2.2 Behavioral effects of intranasal Aβ1-42

Aβ1-42 peptide that was nasally administered induced behavioral changes specific to long-term learning and memory. The behavioral profile of these animals is similar to that observed in case of entorhinal model: slower spatial learning in the Morris water maze test, no changes in short-term memory and in anxiety levels.

The impairment of spatial learning in the Morris water maze test was more pronounced in Experiment 2 (7 days, twice daily administration) than in Experiment 1 (28 days, once daily administration). In healthy mammals, the transporters low density lipoprotein-related protein 1 and P-glycoprotein, present at the blood-brain barrier, very effectively pump out Aβ1-42 from brain to blood, thereby regulating Aβ1-42 concentrations in the nervous system (Zlokovic 2005). The fact that according to our behavioral data, more frequent administration seems to be more effective even despite a shorter treatment, may be related to this efflux pump function and clearance of the peptide. With these limitations in mind, manipulation of the BBB or alternative routes to circumvent the BBB can be exploited to enhance the penetration of Aβ1-42 to brain. For instance, increasing the permeability of the BBB by pertussis toxin leads to an increase in the flux of Aβ1-42 from blood to brain (Clifford et al. 2007).

8.2.3 Applicability of intranasal Aβ1-42 administration in rats as an appropriate model of AD

Our data support previous observations showing that the nasal pathway can be used to target bioactive peptides to the CNS. Nasal administration of β-amyloid peptides can represent a potential new method to study amyloid-induced dysfunctions, with the advantages of being not expensive, non-invasive and easy to apply, although application of repeated anaesthesia needs a careful monitoring and analysis for side-effects, toxicity, changes in behavior or neuropathology.

8.3 Final conclusion

Our final conclusion is that entorhinal as well as nasal administration of Aβ1-42 in rats are suitable models of AD for testing drug candidates in the future. Moreover, our results with Aβ1-42 suggest that the nasal route may be also used for administration of drug candidates, especially if they have a similar structure to Aβ. An additional interest of this method in humans is that it is non-invasive and essentially painless, and can be easily and readily administered by the patient or a physician.

9 ACKNOWLEDGEMENTS

I am grateful to my supervisor and my mentor, Zsuzsa Penke for her scientific guidance, encouragement and support throughout my Ph.D. studies.

I would like to express my gratitude to my supervisor at the Department of Medical Chemistry Prof. Botond Penke.

I am grateful to Dr. Mária Deli and Anita Kurunczi for cooperation in our colaboration and their support and suggestions in my work.

I thank Ágnes Kasza, János Horváth, Zsuzsa Frank for their inspiring help in the studies.

I thank the members of the Research Group of Neurodegenerative Disease and Department of Medical Chemistry their help and friendship.

Finally, I am especially thankful to my husband, my parents and all of my family and friends for their love and untiring support during my studies.

The research was supported by grants from the Hungarian Research Fund (OTKA T37834, T37956, M036252) and the National Office for Research and Technology (RET 08/2004, GVOP-KMA-52).

10 REFERENCES

Aggleton JP, Vann SD, Oswald CJ, Good M (2000) Identifying cortical inputs to the rat hippocampus that subserve allocentric spatial processes: A simple problem with a complex answer. Hippocampus 10:466–474.

Andrade X, Radhakrishnan R, (2009) The prevention and treatment of cognitive decline and dementia: An overview of recent research on experimental treatments. Indian J Psychiatry 51:12-25.

Arendash GW, King DL, Gordon MN, Morgan D, Hatcher JM, Hope CE, Diamond DM (2001) Progressive, age-related behavioral impairments in transgenic mice carrying both mutant amyloid precursor protein and presenilin-1 transgenes. Brain Res 891:42-53.

Banks WA, Robinson SM, Verma S, Morley JE (2003) Efflux of human and mouse amyloid beta proteins 1-40 and 1-42 from brain: impairment in a mouse model of Alzheimer's disease. Neurosci 121:487-492.

Bhatt DH, Zhang S, Gan WB (2009) Dendritic spine dynamics. Annu Rev Physiol Berlin 71:261282. Review.

Blozovski D, Hess C (1989) Hippocampal nicotinic cholinergic mechanisms mediate spontaneous alternation and fear during ontogenesis but not later in the rat. Behav Brain Res 35:209–220.

Braak H, Braak E (1991) Neuropathological stageing of Alzheimer-related changes. Acta Neuropathol 82:239-259. Review.

Broadbent NJ, Squire LR, Clark RE (2004) Spatial memory, recognition memory, and the hippocampus. Proc Natl Acad Sci U S A 101:14515-14520.

Canto CB, Wouterlood FG, Witter MP (2008) What does the anatomical organization of the entorhinal cortex tell us? Neural Plast doi: 10.1155/2008/381243.

Casamenti F, Prosperi C, Scali C, Giovannelli L, Pepeu G (1998) Morphological, biochemical and behavioural changes induced by neurotoxic and inflammatory insults to the nucleus basalis. Int J Dev Neurosci.7 16:705-714. Review.

Chacon MA, Barria MI, Soto C, Inestrosa NC (2004) Beta-sheet breaker peptide prevents abeta-induced spatial memory impairments with partial reduction of amyloid deposits. Mol Psychiatry 9: 953-961.

Cleary JP, Walsh DM, Hofmeister JJ, Shankar GM, Kuskowski MA, Selkoe DJ, Ashe KH (2005) Natural oligomers of the amyloid-beta protein specifically disrupt cognitive function. Nat Neurosci 8:79–84.

Clifford PM, Zarrabi S, Siu G, Kinsler KJ, Kosciuk MC, Venkataraman V, D'Andrea MR, Dinsmore S, Nagele RG (2007) Abeta peptides can enter the brain through a defective blood–brain barrier and bind selectively to neurons. Brain Res 1142:223–236.

Deli MA (2009) Potential use of tight junction modulators to reversibly open membranous barriers and improve drug delivery. Biochem Biophys Acta 1788:892-910.

De Ferrari GV, Chacon MA, Barria MI, Garrido JL, Godoy JA, Olivares G, Reyes AE, Alvarez A, Bronfman M, Inestrosa NC (2003) Activation of wnt signaling rescues neurodegeneration and behavioral impairments induced by beta-amyloid fibrils. Mol Psychiatry 8:195–208.

Degroot A, Parent MB (2000) Increasing acetylcholine levels in the hippocampus or entorhinal cortex reverses the impairing effects of septal GABA receptor activation on spontaneous alternation. Learn Mem 7:293–302.

Dodart JC, May P (2005) Overview on rodent models of Alzheimer's disease. Curr Protoc Neurosci Chapter 9 Unit 9.22.

Duyckaerts C, Delatour B, Potier M (2009) Classification and basic pathology of Alzheimer disease. Acta Neuropathol 118:5–36.

Findeis MA (2007) The role of amyloid β peptide 42 in Alzheimer's disease. Pharma & Therap 116:266–286.

Frankland PW, Bontempi B (2005) The organization of recent and remote memories. Nat Rev Neurosci 6:119-130. Review.

Forwood SE, Winters B, Bussey TJ (2005) Hippocampal lesions that abolish spatial maze performance spare object recognition memory at delay of up to 48 hours. Hippocampus 15:347-355.

Galani R, Weiss I, Cassel JC, Kelche C (1998) Spatial memory, habituation, and reactions to spatial and nonspatial changes in rats with selective lesions of the hippocampus, the entorhinal cortex orthe subiculum. Behav Brain Res 96:1–12.

Hardy JA and Higgins GA (1992) Alzheimer's Disease: The Amyloid Cascade Hypothesis. Science 256:184-185.

Hardy J and Selkoe DC (2002) The amyloid hypothesis of Alzheimer's disease: progress and problems on the road to therapeutics. Science 297:353-356.

Hardy J (2009) The amyloid hypothesis for Alzheimer's disease: a critical reappraisal. J Neurochem 110:1129-1134. Review.

Hartman RE, Izumi Y, Bales KR, Paul SM, Wozniak DF, Holtzman DM (2005) Treatment with an amyloid-beta antibody ameliorates plaque load, learning deficits, and hippocampal long-term potentiation in a mouse model of Alzheimer's disease. J Neurosci 25:6213–6220.

Heinemann U, Schmitz D, Eder C, Gloveli T (2000) Properties of entorhinal cortex projectioncells to the hippocampal formation. Ann N Y Acad Sci 911: 112-126.

Hetényi A, Fülöp L, Martinek TA, Wéber E, Soós K, Penke B (2008) Ligand-induced flocculation of neurotoxic fibrillar Aβ(1–42) by noncovalent crosslinking. Chembiochem 9:748-757.

Horvát S, Fehér A, Wolburg H, Sipos P, Veszelka S, Tóth A, Kis L, Kurunczi A, Balogh G, Kürti L, Erős I, Szabó-Révész P, Deli MA (2009) Sodium hyaluronate as a mucoadhesive componentin nasal formulation enhances delivery of molecules to braintissue. Eur J Pharm Biopharm 72:252–259.

Iadecola C (2003) Cerebrovascular effects of amyloid-beta peptides: mechanisms and implications for Alzheimer's dementia. Cell Mol Neurobiol 23:681-689.

Illum L (2000) Transport of drugs from the nasal cavity to the central nervous system. Eur J Pharm Sci 11:1–18.

Illum L (2004) Is nose-to-brain transport of drugs in man a reality? J Pharm Pharmacol 56:3–17.

Iqbal K, Alonso Adel C, Chen S, Chohan MO, El-Akkad E, Gong CX, Khatoon S, Li B, Liu F, Rahman A, Tanimukai H, Grundke-Iqbal I (2005) Tau pathology in Alzheimer disease and other tauopathies. Biochim Biophys Acta 1739:198-210. Review.

Iqbal K, Liu F, Gong CX, Alonso Adel C, Grundke-Iqbal I (2009) Mechanisms of tau-induced neurodegeneration. Acta Neuropathol 118:53-69. Review.

Janelsins MC, Mastrangelo MA, Oddo S, LaFerla FM, Federoff HJ, Bowers WJ (2005) Early correlation of microglial activation with enhanced tumor necrosis factor-alpha and monocyte chemoattractant protein-1 expression specifically within the entorhinal cortex of triple transgenic Alzheimer's disease mice. J Neuroinflammation 2:23.

Juhász G, Márki A, Vass G, Fülöp L, Budai D, Penke B, Falkay G, Szegedi V (2009) An intraperitoneally administered pentapeptide protects against Abeta (1-42) induced neuronal excitation in vivo. J Alzheimers Dis 16:189-196.

Kandel ER, Schwarz JH, Jessel TM (2000) The principles of Neural Science 4th edition.

Kar S, Slowikowski SP, Westaway D, Mount HT (2004) Interactions between beta-amyloid and central cholinergic neurons: Implications for alzheimer's disease. J Psychiatry Neurosci 29: 427-441.

Kayed R, Glabe CG (2006) Conformation-dependent anti-amyloid oligomer antibodies. Methods Enzymol 413: 326-344.

Kopniczky Z, Dochnal R, Macsai M, Pal A, Kiss G, Mihaly A, Szabo G (2006) Alterations of behavior and spatial learning after unilateral entorhinal ablation of rats. Life Sci 78: 2683-2688.

Lahiri DK, Greig NH (2004) Lethal weapon: Amyloid beta-peptide, role in the oxidative stress and neurodegeneration of alzheimer's disease. Neurobiol Aging 25: 581-587.

Lalonde R (2002) The neurobiological basis of spontaneous alternation. Neurosci Biobehav Rev 26:91–104.

Morrissette DA, Parachikova A, Green KN, LaFerla FM (2009) Relevance of transgenic mouse models to human Alzheimer disease. J Biol Chem 284:6033-6037.

Mucke L (2009) Neuroscience: Alzheimer's disease Nature 461:895-897.

Mumby DG, Pinel JP (1994) Rhinal cortex lesions and object recognition in rats. Behav Neurosci 108:11–18.

Mumby DG (2001) Perspectives on object-recognition memory following hippocampal damage: Lessons from studies in rats. Behav Brain Res 127:159–181.

Nag S, Tang F (1998) Cholinergic lesions of the rat brain by ibotenic acid and 192 IgG-saporin: effects on somatostatin, substance P and neuropeptide Y levels in the cerebral cortex and the hippocampus. Neurosci Lett 252:83–86.

Nitta A, Itoh A, Hasegawa T, Nabeshima T (1994) Beta-amyloid protein-induced Alzheimer's disease animal model. Neurosci Lett 170:63–66.

Nivsarkar M, Banerjee A, Padh H (2008) Cyclooxygenase inhibitors: a novel direction for Alzheimer's management. Pharmacol Rep 60:692-698.

Pardridge WM (2005) The blood-brain barrier: bottleneck in brain drug development. NeuroRx 2:3-14.

Parron C, Poucet B, Save E (2004) Entorhinal cortex lesions impair the use of distal but not proximal landmarks during place navigation in the rat. Behav Brain Res 154: 345-352.

Paxinos G, Watson C (1982) The rat brain in stereotaxic coordinates. New York.

Poucet B, Lenck-Santini PP, Paz-Villagran V, Save E (2003) Place cells, neocortex and spatial navigation: A short review. J Physiol Paris 97: 537-546.

Puoliväli J, Wang J, Heikkinen T, Heikkilä M, Tapiola T, van Groen T, Tanila H (2002) Hippocampal A beta 42 levels correlate with spatial memory deficit in APP and PS1 double transgenic mice. Neurobiol Dis 9:339-347.

Sastre M, Klockgether T, Heneka MT (2006) Contribution of inflammatory processes to Alzheimer's disease: Molecular mechanisms. Int J Dev Neurosci 24:167–176.

Seabrook TJ, Bloom JK, Iglesias M, Spooner ET, Walsh DM, Lemere CA (2004) Species-specific immune response to immunization with human versus rodent A beta peptide. Neurobiol Aging 25:1141–1151.

Selkoe DJ (1991) The Molecular pathology of Alzeheimer's Disease. Neuron 6:487-498. Review.

Selkoe DJ (2001) Alzheimer's disease: genes, proteins, and therapy. Physiol Rev 81:741-766.

Selkoe DJ, Podlisny MB (2002) Deciphering the genetic basis of Alzheimer's disease. Annu Rev Genomics Hum Genet 3:67-99.

Seward TV, Seward A (2003) Input and output station of the entorhinal cortex: superficial vs. Deep layers of lateral vs. medial divison? Brain Reserch Reviews 42:243-251.

Shapiro M (2001) Plasticity, hippocampal place cells, and cognitive maps. Arch Neurol 58:874-881.

Shen YX, Wei W, Yang J, Liu C, Dong C, Xu SY (2001) Improvement of melatonin to the learning and memory impairment induced by amyloid beta-peptide 25–35 in elder rats. Acta Pharmacol Sin 22:797–803.

Siegel A. and Sapru HN (2006) Essential Neuroscience, First Edition.

Simon P, Dupuis R, Costentin J (1994) Thigmotaxis as an index of anxiety in mice. Influence of dopaminergic transmissions. Behav Brain Res 61: 59-64.

Spowart-Manning L, van der Staay FJ (2005) Spatial discriminationdeficits by excitotoxic lesions in the Morris water escape task. Behav Brain Res 156:269–276.

Squire LR, Stark CE, Clark RE (2004) The medial temporal lobe Annu. Rev. Neurosci 27:279–306.

Stephan A, Laroche S, Davis S (2003) Learning deficits and dysfunctional synaptic plasticity induced by aggregated amyloid deposits in thedentate gyrus are rescued by chronic treatment with indomethacin.
Eur J Neurosci 17:1921–1927.

Stephan A, Phillips AG (2005) A case for a non-transgenic animal model of Alzheimer's disease. Genes Brain Behav 4:157-172.

Thal DR, Rub U, Schultz C, Sassin I (2000) Ghebremedhin E., Del Tredici K., Braak E., Braak H. Sequence of abeta-protein deposition in the the human medial temporal lobe. J Neuropathol Exp Neurol, 59: 733-748
Thal DR, Rub U, Orantes M, Braak H (2002) Phases of A-beta deposition in the human brain and its relevance for the development of AD. Neurol 58:1791–1800.

Thompson RF and Kim, JJ (1996) Memory systems in the brain and localization of memory. Proc Natl Acad Sci USA 93:13438-13444.

Thorne RG, Pronk GJ, Padmanabhan V, Frey WH (2004) Delivery of insulin-like growth factor-I to the rat brain and spinal cord along olfactory and trigeminal pathways following intranasal administration. Neurosci 127: 481–496.

Tran MH, Yamada K, Nabeshima T (2002) Amyloid beta-peptide induces cholinergic dysfunction and cognitive deficits: A minireview. Peptides 23:1271-1283.

Van den Berg MP, Verhoef JC, Romeijn SG, Merkus FW (2004) Uptake of estradiol or progesterone into the CSF following intranasal and intravenous delivery in rats. Eur J Pharm Biopharm 58:131-135.

Vehmas AK, Kawas CH, Stewart WF, Troncoso JC (2003) Immune reactive cells in senile plaques and cognitive decline in Alzheimer's disease. Neurobiol Aging 24:321–331.

Wang ZL, Cheng SM, Ma MM, Ma YP, Yang JP, Xu GL, Liu XF (2008) Intranasally delivered bFGF enhances neurogenesis in adult rats following cerebral ischemia. Neurosci Letters 446:30-35.

Wilson DA and Linser C (2008) Neurobiology of a simple memory J Neurophysiol 100:2-7.

Wilson DA, Best AR., Sullivan RM (2004) Plasticity in the Olfactory System: Lessons for the Neurobiology of Memory. Neuroscientist 10:513–524.

Wolburg H, Wolburg-Buchholz K, Sam H, Horva´t S, Deli MA, Mack AF (2008) Epithelial and endothelial barriers in the olfactory region of the nasal cavity of the rat. Histochem Cell Biol 130: 127–140.

Wolfer DP, Stagljar-Bozicevic M, Errington ML, Lipp HP (1998) Spatial Memory and Learning in Transgenic Mice: Fact or Artifact? News Physiol 13:118-123.

Yamada K, Tanaka T, Senzaki K, Kameyama T, Nabeshima T (1998) Propentofylline improves learning and memory deficits in rats induced by beta-amyloid protein-(1-40). Eur J Pharmacol 349:15-22.

Zarandi M, Soos K, Fulop L, Bozso Z, Datki Z, Toth GK, Penke B (2007) Synthesis of abeta[1-42] and its derivatives with improved efficiency. J Pept Sci 13: 94-99.

Zhang Q, Jiang X, Jiang W, Lu W, Su L, Shi Z (2004) Preparation of nimodipine-loaded microemulsion for intranasal delivery and evaluation on the targeting efficiency to the brain. Int J Pharm 275: 85–96.

Zlokovic BV (2005) Neurovascular mechanisms of Alzheimer's neurodegeneration. Trends Neurosci 28:202–208.

11 APPENDIX